Clim. Past Discuss., https://doi.org/10.5194/cp-2018-153
Manuscript under review for journal Clim. Past
Discussion started: 21 November 2018

Climate of the Past Discussions
Open Access
EGU

Towards understanding potential atmospheric contributions to abrupt climate changes: Characterizing changes to the North Atlantic eddy-driven jet over the last deglaciation

Heather J. Andres[1] and Lev Tarasov[1]

[1]Memorial University of Newfoundland, St. John's, NL, CANADA

Correspondence: Heather J. Andres (handres@mun.ca)

Abstract. Abrupt climate shifts of large amplitude were common features of the Earth's climate as it transitioned into and out of the last full glacial state approximately twenty thousand years ago, but their causes are not yet established. Mid-latitudinal atmospheric dynamics may have played an important role in these oscillations through their effects on heat and precipitation distributions, sea ice extent, and wind-driven ocean circulation patterns. This study characterises deglacial winter wind changes over the North Atlantic (NAtl) in a suite of transient deglacial simulations we performed using the PlaSim earth system model, as well as in the TraCE-21ka simulation. We detect multiple instances of NAtl jet transitions that occur within 10 simulation years and a sensitivity of the jet to background climate conditions. Thus, we suggest that changes to the NAtl jet may play a critical role in abrupt glacial climate oscillations.

We identify two types of simulated wind changes over the last deglaciation. Firstly, the latitude of the NAtl eddy-driven jet shifts northward over the deglaciation in a sequence of distinct steps. Secondly, the variability of the NAtl jet gradually shifts from a Last Glacial Maximum (LGM) state with a strongly preferred jet latitude and a restricted latitudinal range to one with no single preferred latitude and a range that is at least 11° broader. Changes to the position of the NAtl jet alters the location of the wind forcing driving oceanic surface gyres and the limits of sea ice extent, whereas a shift to a more variable jet reduces the effectiveness of the wind forcing at driving surface ocean transports.

The processes controlling these two types of changes differ on the upstream and downstream ends of the NAtl eddy-driven jet. On the upstream side over eastern North America, the elevated ice sheet margin acts as a physical barrier to the winds in both the PlaSim simulations and the TraCE-21ka experiment. This constrains both the position and the latitudinal variability of the jet at LGM, so the jet shifts in sync with ice sheet margin changes. In contrast, the downstream side over the eastern NAtl is more sensitive to the thermal state of the background climate. Our results suggest that knowing the position of the south-eastern margin of the North American ice complex strongly constrains the deglacial position of the jet over eastern North America and the western North Atlantic as well as its variability.

Copyright statement.

Clim. Past Discuss., https://doi.org/10.5194/cp-2018-153
Manuscript under review for journal Clim. Past
Discussion started: 21 November 2018

1 Introduction

The last deglaciation encompassed a period of large-scale global warming of the Earth's surface climate, with regional patterns of millennial-timescale oscillations detected in oxygen isotopes in Greenland ice and surface ocean temperatures (Blunier et al., 1998; Shakun and Carlson, 2010; Clark et al., 2012). The Oldest Dryas (OD, 19-14.7ka BP, which includes Heinrich Stadial 1, 17.5-14.7ka BP), the Bølling-Allerød (B-A, 14.7-12.8ka BP), and the Younger Dryas (YD, 12.8-11.7ka BP) describe consecutive periods of stadial and interstadial conditions with rapid adjustments between them (Hammer et al., 1986; Grachev and Severinghaus, 2005; Clark et al., 2012). Signatures of these oscillations are present in the mid- to high-latitudes of both hemispheres with increasing amplitude toward the poles, although the sign tends to be anti-phased between the two hemispheres and of lower amplitude in the south (Shakun and Carlson, 2010). Such oscillations are also present in proxy indicators for variables other than temperature. Ocean circulation proxies indicate a deepening of the Atlantic Meridional Overturning Circulation (AMOC) and a northward shift in the northern boundary of the subtropical gyre with shifts from stadial to interstadial conditions in northern high latitudes (and vice versa) (e.g. Gherardi et al. (2009); Clark et al. (2012); Repschläger et al. (2015)). Abrupt shifts have also been detected in reconstructed lake levels and speleothem data in the subtropics and Indian and African monsoon regions, suggesting latitudinal shifts of the InterTropical Convergence Zone (ITCZ) (e.g. Jacob et al. (2007) and Mohtadi et al. (2016)).

Proposed hypotheses explaining the presence of such oscillations commonly centre around deep-ocean circulation changes in response to salinity anomalies in the regions of deepwater formation.Different freshwater sources have been proposed to generate an abrupt reduction in the AMOC: changes in regional discharge from North American ice sheets (Rooth, 1982; Broecker et al., 1989; Tarasov and Peltier, 2005; Keigwin et al., 2018), increased freshwater export from the Arctic in response to the opening of the Bering Strait (Hu et al., 2010), and export of thick sea ice from the Arctic basin (Bradley and England, 2008). In climate model simulations, slowing down the AMOC using freshwater sources can provide an effective way of generating abrupt cooling in the extratropical North Atlantic (NAtl), Nordic Seas, Arctic and Eurasia, as well as reducing precipitation in the NAtl, Europe and African and Indian monsoon regions (Kageyama et al., 2010, 2013). Southward shifts of the ITCZ in the Atlantic basin have also been detected in response to simulated AMOC reductions (Kageyama et al., 2010, 2013). However, reducing freshwater fluxes is less effective at generating abrupt warmings such as were observed at the start of the B-A and the end of the YD (Kageyama et al., 2010). If AMOC changes occur at least in part from hysteresis under the gradually-changing background conditions of the last deglaciation or through internal variability of the climate, rather than solely freshwater surges, then abrupt changes in either direction are possible (Knorr and Lohmann, 2007; Kageyama et al., 2010; Peltier and Vettoretti, 2014). Nevertheless, AMOC changes alone may be insufficient to explain all aspects of the abrupt changes during the last deglaciation, as corresponding warming in the South Atlantic and Southern oceans do not always accompany simulated AMOC reductions (Kageyama et al., 2013) and the amplitude of corresponding simulated signals over Greenland and Europe are smaller than reconstructed (Clark et al., 2012).

Alternative explanations for the abrupt transitions of the last deglaciation include thermohaline circulation responses as a single aspect of more complex mechanisms (Seager and Battisti, 2007), or that changes in wind fields played the central role

Clim. Past Discuss., https://doi.org/10.5194/cp-2018-153
Manuscript under review for journal Clim. Past
Discussion started: 21 November 2018

(Wunsch, 2006). For example, altered winter sea ice extent is sufficient to reproduce the amplitude of deglacial climate oscillations in northwestern Europe and explain their seasonality (Renssen and Isarin, 2001). Winter sea ice cover today is constrained by low-level wind patterns over the Arctic and Greenland (Venegas and Mysak, 2000) and surface ocean heat transports in the NAtl (themselves affected by wind forcing over the NAtl) (Lozier et al., 2010; Häkkinen et al., 2011; Li and Born)). During the deglaciation, changes to the variability of low-level winds can alter gyre transports (and to a lesser degree, wind position and strength), as highly variable winds are less effective at transporting surface water via Sverdrup transport than steady winds (Li and Born). A stronger and more eastwardly extensive subpolar gyre restricts the transport of warm, salty water northward from the subtropical gyre, which also affects rates of deepwater formation (Häkkinen et al., 2011; Muglia and Schmittner, 2015). Thus, deglacial, winter wind conditions over the North Atlantic may have played important roles in the detected abrupt climate oscillations through their effects on sea ice and/or the surface ocean circulations.

Of the two dominant features of mid-latitude atmospheric circulation patterns in the NAtl, the subtropical and eddy-driven jets, the eddy-driven jet has the largest presence at low levels of the atmosphere. The eddy-driven jet (or polar front jet or jet stream) is a narrow band of fast, westerly winds that arises from the convergence of atmospheric synoptic-scale eddies (e.g. extratropical cyclones with lifespans of days) (Lee and Kim, 2003; Barnes and Hartmann, 2011). These baroclinic eddies are primarily created by the strong temperature gradients along the boundary between polar and tropical air masses and/or the wind shear on the flank of the subtropical jet (Lee and Kim, 2003; Justino et al., 2005). Since these two phenomena occur at different latitudes, the position of the eddy-driven jet depends on their relative strengths (Lee and Kim, 2003):

- under a weak subtropical jet as in the NAtl today, the eddy-driven jet tends to be distinct from the subtropical jet and located in the mid-latitudes;
- under a strong subtropical jet as in the North Pacific (NPac) today, the eddy-driven jet tends to lie along the poleward flank of the subtropical jet in a "merged" state.

Additional eddy sources that localize the eddy-driven jet in longitude as well as latitude include the baroclinicity of land-sea boundaries or other surface temperature gradients, and the breaking of Rossby waves (see Box 1 of Cohen et al. (2014) for an overview of the phenomena affecting and affected by the eddy-driven jet). Due to the greater temperature contrasts between equator and pole or land and sea during a hemisphere's winter, the eddy-driven jet is stronger and more localized during winter. Summer changes to the winds and climate during the deglaciation are of primary importance to the rates and locations of ice sheet melt and retreat. However, the eddy-driven yet is strongest in the winter and is therefore more likely to impact the rest of the atmosphere/ocean system during that season. As such, we restrict our attention in this study to the northern winter, or DJF.

Since the eddy-driven jet's position depends on the characteristics of the eddy field, any changes to locations or rates of eddy production and decay will change the jet. However, the jet itself is a source of eddies in the form of midlatitude cyclones, or storm tracks. Thus, variations in the jet's position over time arise from complex process of feedback interactions between changes to eddies generated by the background climate, and changes to the eddies arising from the jet's response (Cohen et al., 2014). The type of variability depends on the latitudinal position of the jet. Eddy-driven jets located closer to the equator (and the subtropical jet) or the pole tend to vary in strength (pulse) while jets in the central midlatitudes tend to meander latitudinally

Clim. Past Discuss., https://doi.org/10.5194/cp-2018-153
Manuscript under review for journal Clim. Past
Discussion started: 21 November 2018

(Barnes and Hartmann, 2011). Depending on the type of variability, the patterns of heat and moisture transported by the jet will be either concentrated to a narrow band of latitudes around the jet's mean position or spread over a large area.

Under LGM boundary conditions, with ice sheet cover extending to the mid-latitudes over North America (NAmer) and over Fennoscandia (Dyke, 2004; Hughes et al., 2016), both the position of the ITCZ (and presumably the subtropical jet) (Arbuszewski et al., 2013) and the regions of baroclinicity are different from present-day. The topographic and thermal barriers presented by the ice sheet complex over NAmer, in particular, alter the stationary wave field, the pattern of transient eddy production and decay, and the locations of baroclinic zones around the NH (Rind, 1987; Cook and Held, 1988; Roe and Lindzen, 2001a, b; Justino et al., 2005; Li and Battisti, 2008; Lofverstrom et al., 2014; Merz et al., 2015). These effects have their strongest manifestation just downstream of the North American Ice Sheet complex (NAIS), in the NAtl. However, the influences on the western and eastern sides of the NAtl have been found to differ in atmospheric simulations, whereby the position of the western side of the jet is more affected by orography and the position of the eastern side of the jet is primarily influenced by transient eddies (Kageyama and Valdes, 2000). While the routing of storm tracks and the jet's contribution to poleward atmospheric heat transport may be most affected by the behaviour of the jet over the eastern NAtl, the position of the western side of the jet over eastern NAmer is of particular importance to the wind-driven ocean circulation through Sverdrup transport (Li and Born). Given the above and that there is no reason to expect equal and synchronous changes in eastern and western NAtl jet positions over deglaciation, both positions should be diagnosed. Following the convention in recent literature, we also use the jet's mean latitudinal position and its east-west difference in latitudinal position (differencing regions marked by black boxes in Figure 4), or its tilt, as additional metrics.

NAtl eddy-driven jet characteristics in LGM simulations for multiple models from the Paleoclimate Modelling Intercomparison Project (PMIP) 3 show little consistency, except that the jets are all stronger and less variable than in corresponding preindustrial simulations (P. Hezel, personal communication). However, in simulations based on the NCAR family of models (CCSM3, CCSM4 and their components), the NAtl eddy-driven jet at LGM follows a less tilted path and is stronger and less latitudinally-variable than at present (Li and Battisti, 2008; Lofverstrom et al., 2014; Merz et al., 2015). These changes are consistent with the NAtl eddy-driven jet entering the aforementioned "merged" state at LGM, which corresponds to a reduction in the transport of heat to and precipitation over the British Isles and Fennoscandia (Li and Battisti, 2008; Lofverstrom et al., 2014; Merz et al., 2015).Sometime during the last deglaciation, the pattern and variability of simulated midlatitude winds must change, especially in response to the ice sheet topography changes (Cook and Held, 1988; Rind, 1987; Justino et al., 2005; Li and Battisti, 2008; Merz et al., 2015). However, there is little information as to whether these changes occurred at the time of the climate oscillations. In the TraCE-21ka deglacial simulation Liu et al. (2009); He (2011); Liu et al. (2012), the NAtl jet exhibits two characteristic states: a strong, stable, zonal glacial jet and a weaker, latitudinally-variable, tilted interglacial jet (Lofverstrom and Lora, 2017). The transition from the one jet state to the other is abrupt and coincident with the separation of the Cordilleran and Laurentide ice sheets at 13.89 ka BP (Lofverstrom and Lora, 2017). This timing would place the abrupt change during the middle of the B-A, which would rule out its playing an important, proximal role in triggering abrupt climate oscillations during the last deglaciation. However, their study employed only a single simulation forced by the ICE-5G ice sheet reconstruction, which over-predicts the height of the Keewatin dome with respect to more recent reconstructions (Tarasov et al.,

Clim. Past Discuss., https://doi.org/10.5194/cp-2018-153
Manuscript under review for journal Clim. Past
Discussion started: 21 November 2018

2012; Peltier et al., 2015) and is inconsistent with present-day uplift data (Tarasov and Peltier, 2004). This study diagnoses the changes undergone by the NAtl eddy-driven jet from the LGM to the preindustrial period in multiple transient deglacial experiments using a newer ice sheet reconstruction without prescribed meltwater fluxes. These simulations are performed using a modified version of the Planet Simulator (PlaSim) version 16, a simplified Earth System Model with a primitive equation atmosphere (Lunkeit et al., 2012), and transient boundary conditions following the specifications of the PMIP4 (Ivanovic et al., 2016). As such, these simulations can provide an important comparison against PMIP4 deglacial studies performed using more complex models and help elucidate whether atmospheric dynamical changes have the potential to play important roles in the abrupt climate changes of the last deglaciation.

2 Methods

The experiments discussed in this paper consist of four transient simulations of the last deglaciation using a modified version of PlaSim and a suite of sensitivity studies (FixedOrbGHG, FixedGlac, PDTopo and DarkGlac). A subset of the same boundary conditions and initial conditions are applied in all of the fully transient experiments, which are described in Table 1. Ensemble members differ by the radiation parameter set used, all of which were identified as optimized configurations for reproducing radiative fields during the preindustrial period. Further details of the tuning procedure are available in Supplemental Section S1.0.1.

The goals of the sensitivity experiments are to isolate the contributions of ice sheet height, ice sheet albedo, and orbital and GHG forcings to the jet changes we detect, by fixing one forcing at a time and running otherwise identical simulations over the entire deglaciation. Each sensitivity experiment was repeated for all tuning configurations employed in the fully-transient experiments. Note that the results of the DarkGlac experiments were not significantly different than the fully-transient runs due to the reflectivity of snow on top of the dark ice, so their results are not discussed.

Characteristics of PlaSim are described in Section 2.1, and the model's performance at simulating LGM climate is described in Section 2.2.5. Finally, the boundary conditions are described in Section 2.2.

2.1 Planet Simulator

PlaSim consists of the Portable University Model of the Atmosphere (PUMA) wet primitive equation atmosphere model, the Simulator for Biospheric Aspects (SIMBA) dynamic vegetation model, a zero-layer thermodynamic sea ice model, a slab-ocean model and the Large-Scale Geostrophic (LSG) ocean model. PUMA solves the primitive equations. Herein we use a spectral resolution of T42 (approximately 2.8°x2.8°), which has been previously shown to be of sufficiently high resolution to resolve phenomena of interest to the the eddy-driven jet (Barnes and Hartmann, 2011) while enabling fast enough model run times to enable an ensemble of deglacial experiments. The dynamical atmospheric solutions are interpolated to a Gaussian grid that is then used for diabatic calculations, including all other sub-components except for LSG. Thus, for every atmospheric time step, the land, sea ice and slab-ocean components are called sequentially using the same grid and land-sea mask (a schematic is available in Supplemental Figure S1).

Clim. Past Discuss., https://doi.org/10.5194/cp-2018-153
Manuscript under review for journal Clim. Past
Discussion started: 21 November 2018

Climate of the Past Discussions

Table 1. Characteristics of numerical simulations presented in this study. The time-varying forcings are described in section 2.2, and are either transient (T) or fixed (F). Topography includes ice sheet topographic variations as well as corresponding changes to surface roughness and land mask. GHG represents greenhouse changes enacted through effective CO_2 concentrations.

Name	Timespan		Time-varying Forcings			
	Start (BP)	End (BP)	Topography	Land ice albedo	GHG	Orbital
FullyTrans1-4	21000	0	T	T	T	T
FixedOrbGHG1-4	21000	0	T	T	F (LGM)	F (LGM)
FixedGlac1-4	21000	0	F (LGM)	F (LGM)	T	T
PDTopo1-4	21000	0	F (past1000)	T	T	T
DarkGlac1-4	21000	0	T	F (past1000)	T	T

Rather than specifying a fixed deep-ocean heat flux to the mixed layer ocean, PlaSim estimates these fluxes by executing LSG every 32 atmospheric time steps (equivalent to 4.5 days). LSG is run at 2.5°x5° horizontal resolution with a fixed, present-day land-sea mask. LSG solves the primitive equations implicitly for all oceanic layers under assumptions of large spatial and temporal scales (Maier-Reimer et al., 1993). This formulation permits stable solutions on longer time steps than other components of PlaSim with the trade-off that it filters out gravity waves and barotropic Rossby waves (Maier-Reimer et al., 1993). The spatial map of differences between the mixed-layer temperature (Tmix) at the end and the start of the LSG time step are used to define a map of deep-ocean heat fluxes for the slab-ocean model. Thus, under constant atmospheric conditions, the slab ocean model relaxes toward the LSG solution. Under changing atmospheric conditions, the surface component of the ocean will tend toward a mixture of the LSG solution and a thermal response to the surface forcing.

For the experiments performed in this study, the PlaSim model was modified to allow time-varying boundary conditions. Changing boundary conditions include land-sea mask (implemented for all model components except LSG), topography, ice mask, orographic component of surface roughness, orbital configuration and greenhouse gas concentration. Note that although the land mask was altered consistently with changing ice sheet mass, no corresponding salinity anomalies were introduced to the oceans. However, surface runoff routing was recalculated every time the ice sheet configuration changed.

Further details about PlaSim are available in Supplemental Section S1.

2.2 Boundary Conditions

PlaSim boundary conditions are updated every simulation year. For all of the transient simulations presented, the forcings are accelerated by a factor of ten. This acceleration was not found to alter the main conclusions of this study when tested with a single unaccelerated run. More particulars about the differences between the accelerated and unaccelerated runs are presented

Clim. Past Discuss., https://doi.org/10.5194/cp-2018-153
Manuscript under review for journal Clim. Past
Discussion started: 21 November 2018

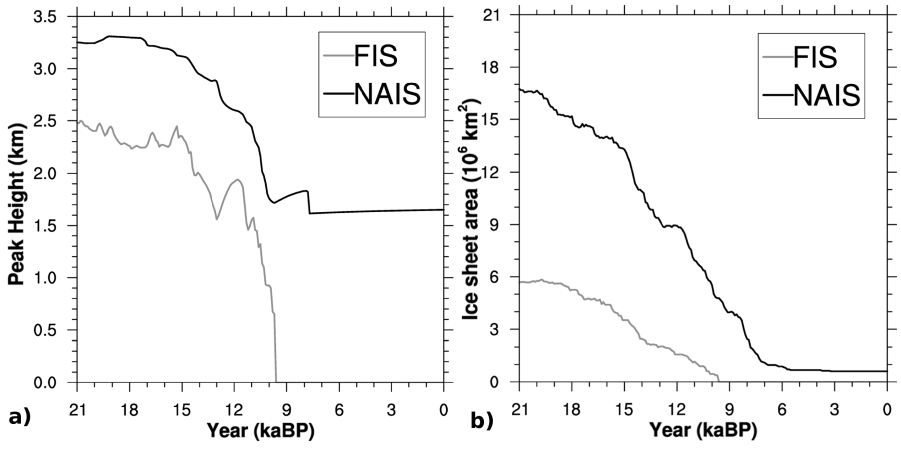

Figure 1. a) Peak ice sheet height and b) area for North America (NAIS) and Eurasia (FIS).

in Appendix section A2. Where the time between boundary condition updates is shorter than the temporal resolution available for a boundary condition dataset, the boundary conditions are linearly interpolated in time. For ice sheet and land-sea masks, the interpolated values are then rounded to zero or one with a cutoff of 0.5.

2.2.1 Land-sea mask, land topography, land-ice mask

Changes in land-sea mask, land topography and land-ice mask are derived from the GLAC1-D deglacial chronology generated with the three-dimensional glacial systems model (GSM) that includes a thermomechanically-coupled ice sheet model, visco-elastic bedrock response, and various other components (cf Tarasov et al., 2012; Briggs et al., 2013, and references therein). The North American (Tarasov et al., 2012) and Eurasian components (Tarasov et al., 2014) are obtained from large ensemble Bayesian inversions against large sets of geophysical and geological observations. The Antarctic component (Briggs et al., 2014) is a best scoring run (against data constraints) from a large ensemble and the Greenland component (Tarasov and Peltier, 2003) is an older hand-tuned model. These four components have then been post-processed to create a gravitationally self-consistent global deglaciation chronology with a temporal resolution of 100 years. These data are interpolated to the model grid, with land-sea mask defined so the topography of ocean grid cells lies below the contemporaneous sea level.

Time series of ice sheet areas and peak heights for North America and Fennoscandia are plotted in Figure 1. In both the North American ice sheet complex (NAIS) and Fennoscandian ice sheet complex (FIS), ice sheet margins begin retreating before peak heights change noticeably. The ice sheet areas decrease approximately linearly, with pauses for both the NAIS and the FIS during the Younger Dryas (approximately 13 to 12ka BP). In contrast, the rate of peak height decrease accelerates with time. Thus, the bulk of peak height changes occur from 12ka BP to 9ka BP. The FIS completely disappears by 9 ka, while a significant Labrador ice dome is present at 8 ka (and largely dissipates by 7 ka).

Clim. Past Discuss., https://doi.org/10.5194/cp-2018-153
Manuscript under review for journal Clim. Past
Discussion started: 21 November 2018

2.2.2 Surface roughness

The component of surface roughness due to orography is calculated from the topography data described above via a similar method to what was used for the default present-day roughness provided with the model (Tibaldi and Geleyn, 1981). For each T42 grid cell, all 0.5°x0.5° ice sheet grid cells contained within it are identified. The variance of the topography of these higher-resolution grid cells are calculated and divided by an effective higher-resolution grid cell length per the T42 grid cell. This effective length is the length of a side of a square whose area is calculated by dividing the area of the T42 model grid cell evenly over the number of high-resolution grid cells within it.

2.2.3 Orbital configuration

Orbital parameters are calculated internally within the model given an orbital forcing year. The equations follow Berger (1978), and the orbital year is updated every simulation year.

2.2.4 Greenhouse gas concentration

The only greenhouse gas explicitly handled in PlaSim is carbon dioxide (CO_2). In this study, other trace gases are accounted for by defining an effective CO_2 concentration value that yields radiative changes equivalent to the combination of CO_2, nitrous oxide (N_2O) and methane (CH_4). Effective CO_2 concentrations were defined with respect to reference CO_2 concentrations at year 22.3ka BP using the equations in Ramaswamy et al. (2001). This reference year was chosen, because both N_2O and CH_4 values were at a relative minimum at that time, and this year precedes the period of interest for our study. Data for CO_2, N_2O and CH_4 concentration changes over the deglaciation are consistent with the prescriptions of the PMIP4 Deglacial experiment (see Ivanovic et al. (2016) and data sources Luthi et al. (2008) Meinshausen et al. (2017), Ivanovic et al. (2016), and Loulergue et al. (2008)). Effective CO_2 concentration values are updated every simulation year, and are linearly interpolated in time between available data points as needed.

2.2.5 Model Evaluation

We compare the climate conditions during the first and last century of the fully-transient PlaSim simulations (forcing years 21-20ka BP and 1ka BP to 1950AD, respectively) to the results of LGM and past1000 experiments in the Climate Modelling Intercomparison Project (CMIP) 5. Only CMIP5 simulations that include experiments using the same model configuration for both LGM and past1000 are included here, as tabulated in Supplementary Table S1.

In Figures 2 and 3, near-surface temperatures (T2m) and sea ice concentrations are plotted for ensemble averages of the first and last centuries of the fully-transient PlaSim simulations. Hatching in Figure 2 indicates where the PlaSim ensemble average T2m lie within the range spanned by the CMIP5 multi-model ensemble members (interpolated to the same resolution). Red and gold lines in Figure 3 identify CMIP5 multi-model ensemble maximum and minimum sea ice extents during the same season, respectively. The surface climate is colder and sea ice more extensive during LGM in the PlaSim simulations than the CMIP5 multi-model ensemble members for both DJF and JJA. This is particularly true in the northern high latitudes, where

Clim. Past Discuss., https://doi.org/10.5194/cp-2018-153
Manuscript under review for journal Clim. Past
Discussion started: 21 November 2018

temperatures over the Arctic Ocean lie below all CMIP5 ensemble members and sea ice is anomalously extensive in the NPac and on the eastern side of the NAtl. In contrast, Antarctic temperatures lie within the range of CMIP5 models, and Southern Ocean sea ice is close to the CMIP5 maximum.

Most of these disagreements are resolved by the past1000, when PlaSim-predicted temperatures and sea ice concentrations lie within the CMIP5 range in most regions. However, temperatures remain anomalously cold over the Arctic during DJF and over oceans in the midlatitudes in both hemispheres and seasons, and sea ice extent exceeds the CMIP5 maximum in the Southern Ocean during JJA. These differences are discussed in more detail in Appendix section A1.

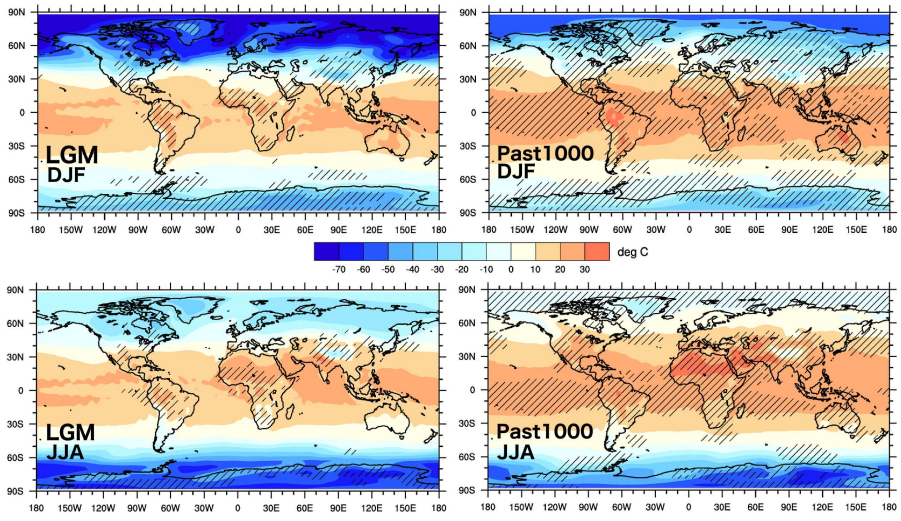

Figure 2. 2m temperatures averaged over all PlaSim ensemble members for indicated seasons and periods. Hatching indicates where the PlaSim ensemble average values lie within the range of CMIP5 models.

Lower-level zonal winds from both PlaSim and CMIP5 averages are plotted in Figure 4 for DJF with the sea ice margin outlined in blue. Zonal winds during the past1000 in the PlaSim simulations lie within the range covered by the CMIP5 multi-model ensemble except over North America and central Eurasia, where winds are stronger in PlaSim. Also, the path of the NPac jet is displaced further north and is more tilted in the PlaSim past1000 simulations. During the LGM, peak zonal winds from PlaSim simulations are stronger than the CMIP5 multi-model ensemble in northern midlatitudes, and the peak winds of the jets are shifted further east toward the the eastern margins of the northern ocean basins. We speculate that this eastern shift is connected to the much more southern extent of sea ice on the eastern side of the NAtl. In spite of these specific differences, the pattern of wind changes from the LGM to the past1000 are similar in both CMIP5 and PlaSim runs (including during JJA, not shown) even though the differences are stronger in the PlaSim transient simulations.

Clim. Past Discuss., https://doi.org/10.5194/cp-2018-153
Manuscript under review for journal Clim. Past
Discussion started: 21 November 2018

Climate of the Past Discussions
Open Access
EGU

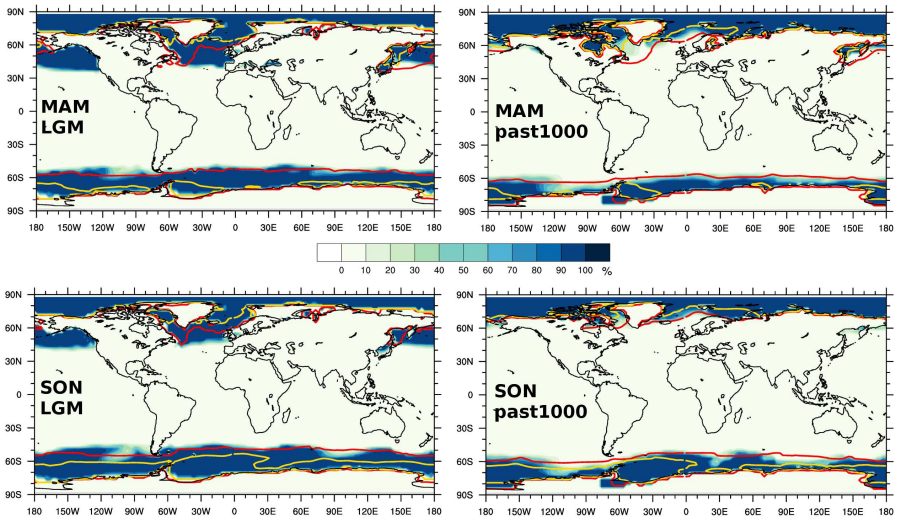

Figure 3. Maps of sea ice concentration averaged over all PlaSim ensemble members for indicated seasons and periods. The CMIP5 multi-model maximum extents denoted by the 15% concentration line are plotted for corresponding seasons and experiments in the red lines. The CMIP5 multi-model minimum extents are plotted in the gold lines.

3 Results and Discussion

3.1 Differences between the LGM and past1000 Climates

We begin by comparing in more detail the characteristics of the NAtl eddy-driven jets during LGM and past1000. The peak winds of the subtropical and eddy-driven jets derived from DJF zonal-wind profiles in Figure 5 occur at similar levels in the upper troposphere during both periods. In contrast, only the eddy-driven jet continues to have a strong influence on winds in the lower troposphere. Therefore, as in Woollings et al. (2010), eddy-driven jet latitudes are defined for the remainder of this analysis to be the location of maximum zonal winds averaged over the NAtl basin within 15°N to 75°N and over atmospheric levels 700hPa to 925hPa. Unlike Woollings et al. (2010), however, these latitudes are defined from monthly data (without low-pass filtering) over longitudes of 90°W to 0°W and are aggregated over 10 consecutive DJF periods to generate jet latitude frequencies. NAtl eddy-driven jet tilt is defined to be the difference between the jet latitudes calculated in the same manner from zonal winds averaged over 90°W to 60°W and 30°W to 0°W.

The NAtl eddy-driven jet in these simulations is stronger, narrower, and shifted equatorward at LGM compared to past1000, according to the profiles of low-level winds in Figure 5 and histograms for the jet latitudes in Figure 6. The mean jet latitude shifts from 41°N to 50°N (with a grid cell length of 2.8°) from LGM to the past1000 in the PlaSim simulations. A shift of the same size is observed on both the upstream and downstream regions of the eddy-driven jet (Figure 7). The lowest latitude occupied by the jet remains unchanged between these two periods, while the highest latitude occupied by the jet increases by 11°. This reflects both an increased range of NAtl eddy-driven jet latitudinal variations as well as an asymmetric change to the

Clim. Past Discuss., https://doi.org/10.5194/cp-2018-153
Manuscript under review for journal Clim. Past
Discussion started: 21 November 2018

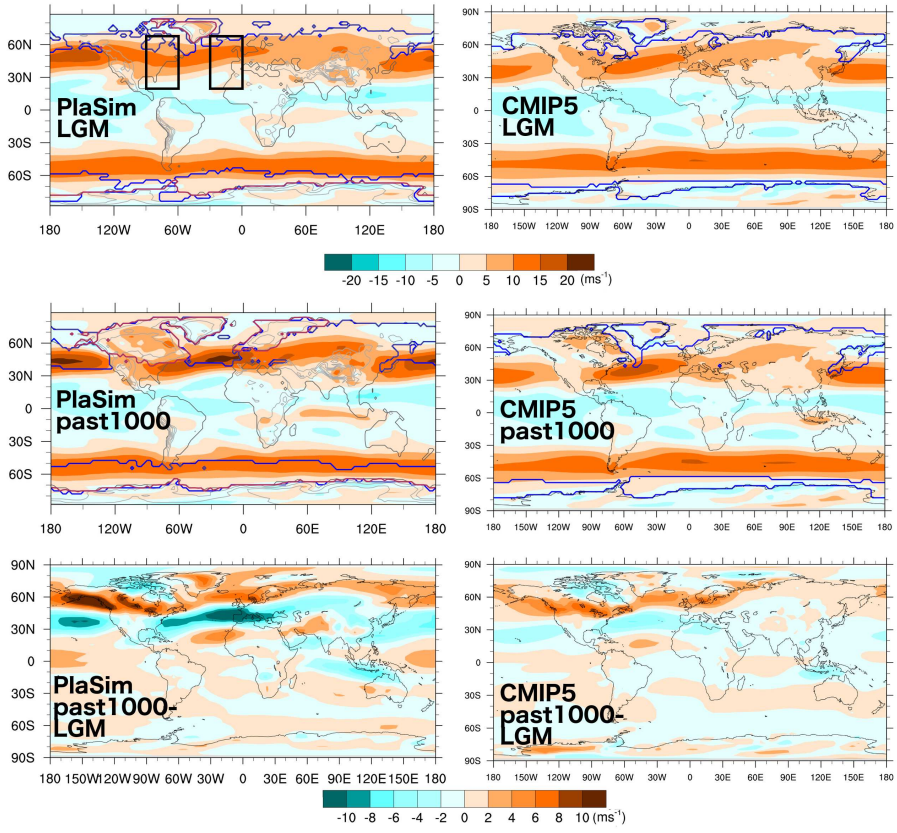

Figure 4. Zonal winds averaged over 700 to 925hPa and averaged over all PlaSim ensemble members or CMIP5 multi-model ensemble members for DJF and indicated periods. Differences between climatologies for these two periods are in the bottom row. Blue lines mark the outline of the 15% concentration line for sea ice, and purple lines mark the land ice mask in PlaSim simulations. Black boxes outline the regions over which the western and eastern components of the NAtl jet are evaluated.

shape of the jet latitudinal distribution. Whereas the jet latitudinal distribution is weakly bimodal at past1000 when calculated over the entire geographic range of the NAtl jet (as in Barnes and Hartmann (2011) and similar to the central and northern positions of Woollings et al. (2010)), it is unimodal at LGM.

In contrast, the mean tilt values in Figure 8 change little from LGM to past1000. Instead, the most prominent difference in the jet tilt between LGM and past1000 is in its distribution: at past1000, the fraction of time that the jet spends in its preferred jet tilt position is smaller and its range of values is larger. This difference reflects a shift away from a single, preferred jet latitude on both the eastern and western sides of the eddy-driven jet, and an increase in the range of both.

The NAtl eddy-driven jet changes from LGM to past1000 in the PlaSim simulations are compared against changes in the only publicly-available fully-transient, coupled deglacial simulation (TraCE-21ka, Liu et al. (2009); He (2011); Liu et al. (2012)) in the right columns of Figures 6 and 8. Jet histograms for TraCE-21ka are calculated in the same way as for the PlaSim

Clim. Past Discuss., https://doi.org/10.5194/cp-2018-153
Manuscript under review for journal Clim. Past
Discussion started: 21 November 2018

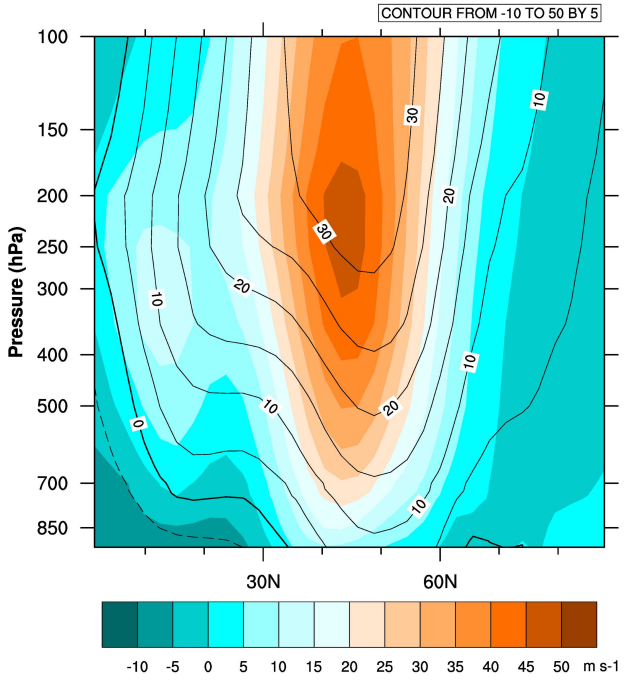

Figure 5. Ensemble average of zonal wind profiles for the NAtl for LGM in coloured contours and past1000 in contour lines.

simulations, except that the data are binned according to the lower resolution of this simulation (T31, equivalent to 3.7° of latitude). Although the mean jet positions and jet distributions over years 1000ka BP to 1950 AD are different between the two datasets, the changes from the LGM to the past1000 are quite similar between TraCE-21ka and the PlaSim ensemble. In TraCE-21ka, the mean jet latitude shifts poleward by approximately 6°, which is less than a grid cell smaller than the change in the PlaSim ensemble. The minimum jet latitude remains unchanged, and the maximum jet latitude expands 18°. The mean tilt for the jet shifts slightly higher in the TraCE-21ka dataset by the past1000, but the most common tilt value remains unchanged from the LGM.

The distributions of jet latitude are not Gaussian in either the PlaSim simulations or the TracE-21ka simulation, so assessing changes to these jet characteristics over the deglaciation via their means and standard deviations can lead to misleading interpretations of the changes that are occurring. Such differences in interpretations can have important implications for heat and moisture transports to the northern NAtl and north-western Europe. Thus, we characterize changes to the distributions of jet attributes as we analyse the simulations over the deglaciation.

3.2 Transitioning from LGM to past1000

None of the transient simulations presented here produce abrupt oscillations between stadial and interstadial conditions at the time of the OD, B-A, and YD. Instead, the accelerated runs all show a single abrupt increase in Greenland temperatures that

Clim. Past Discuss., https://doi.org/10.5194/cp-2018-153
Manuscript under review for journal Clim. Past
Discussion started: 21 November 2018

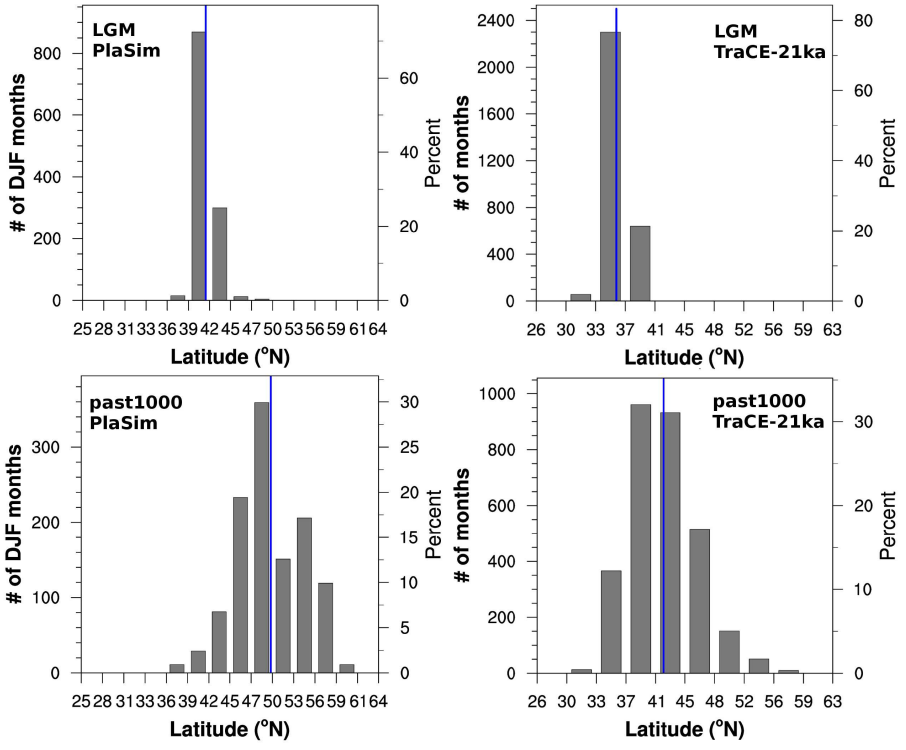

Figure 6. Histograms of latitudes corresponding to peak NAtl zonal winds for all PlaSim ensemble members (left column) and the TraCE-21ka data (right column) during indicated periods. Vertical blue lines indicate mean jet latitudes for the time period.

occurs at different times for each simulation between 12ka BP and 5ka BP. This appears to be a manifestation of internal variability of the model, as the timings of the changes do not coincide between ensemble members and an identically-forced simulation without acceleration exhibits five such abrupt changes over the course of the deglaciation. The characteristics of this phenomenon will be discussed in another paper.

The accelerated transient simulations do show changes in the position, tilt and variability of the NAtl eddy-driven jet, but these changes do not coincide with the large-amplitude climate oscillations. Nevertheless, this absence does not rule out the possibility that jet changes may have played an important role in historical abrupt climate changes via feedbacks between the atmosphere, ocean, land ice and sea ice that are not captured in the simulations here. Thus, we characterize the atmospheric changes present in the accelerated transient simulations and leave assessments of their implications for future work.

The following results are presented via frequency plots that use colour to illustrate the percentage of months in ten successive winter seasons (DJF) that the jet occupies a given latitude band or tilt plotted as a function of latitude and time. Ten years of winters are chosen as a balance between providing sufficient statistics (30 months) to be able to characterise the distribution of jet characteristics and a desire for high temporal resolution to assess the abruptness of changes. Only ensemble statistics are

Clim. Past Discuss., https://doi.org/10.5194/cp-2018-153
Manuscript under review for journal Clim. Past
Discussion started: 21 November 2018

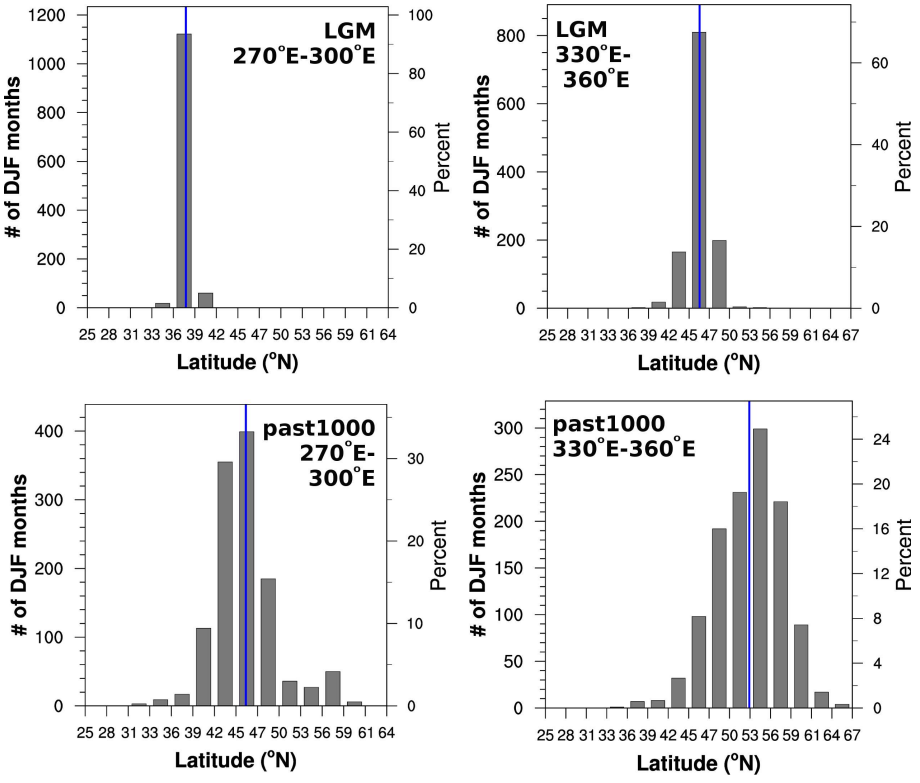

Figure 7. Histograms of latitudes corresponding to peak NAtl zonal winds for all PlaSim ensemble members over the western and eastern regions of the jet during indicated periods. Vertical blue lines indicate mean jet latitudes for the time period.

presented, as deglacial changes over time occurred similarly in all ensemble members. Frequency plots for jet latitude and tilt changes over the deglaciation for each ensemble member individually can be found in Supplemental Figures S2 and S3.

The low-level, NAtl jet exhibits a narrow range of latitudinal variability in the FullyTrans runs at the start of the deglaciation in Figure 9, with the peak winds occurring at the same latitude for more than half of the months. However, the latitude at which the jet is preferentially situated shifts northward three times over the deglaciation in all ensemble members. The shifts occur around 19ka BP, 14ka BP and 11ka BP in all simulations, but the abruptness is not the same for all shifts. The first transition is a gradual one, with a gradual reduction in the frequency of time that the jet spends at the lower latitude at the same time as a gradual increase in the frequency spent at the next grid cell. In contrast, the second and third transitions occur within a decade of simulation (a century of forcing).

A second type of transition is evident in the FullyTrans results in Figure 9, whereby the frequency of time that the NAtl eddy-driven jet spends at its preferred latitude decreases, and the range of jet latitudes increases. This reduction in frequency occurs gradually over a few centuries of simulation, and its timing differs between ensemble members. Note that the development of an isolated northern branch of mean jet latitudes sometime between 15 and 14ka BP in Figure 9 is an artifact due to a computed

Clim. Past Discuss., https://doi.org/10.5194/cp-2018-153
Manuscript under review for journal Clim. Past
Discussion started: 21 November 2018

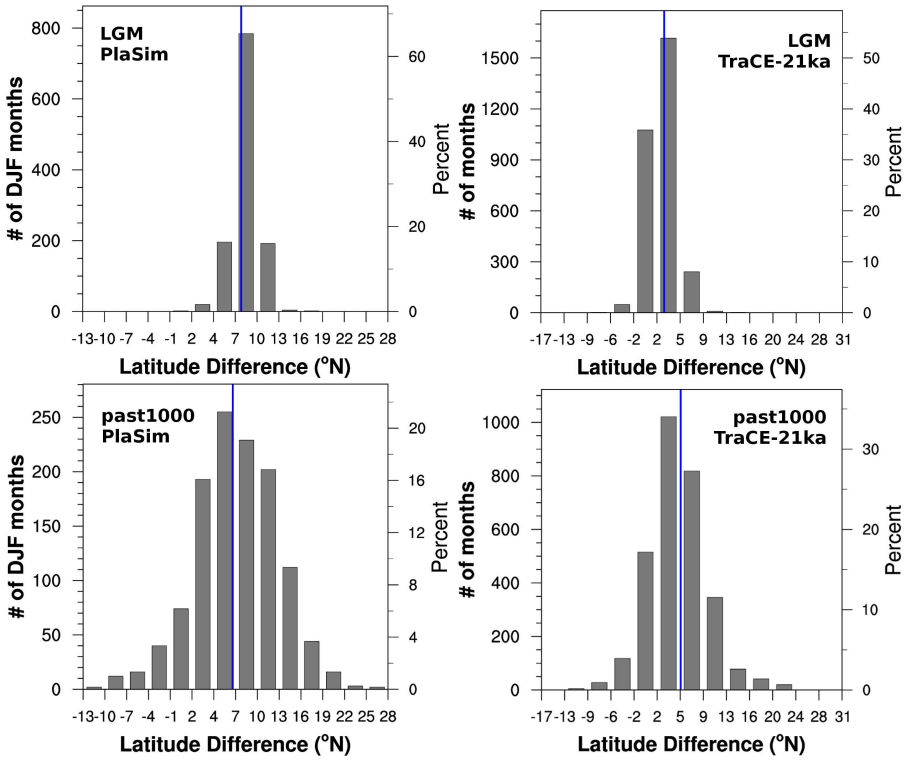

Figure 8. Histograms of jet tilt for the PlaSim ensemble (left column) and TraCE-21ka fully-transient simulation (right column) over indicated periods. Vertical blue lines mark the mean jet tilt for each period.

contribution from a split jet stream over North America. This issue is discussed in more detail in Section 3.3 and Supplemental Section S2.

Ensemble statistics for the NAtl jet tilt in the FullyTrans runs in Figure 9 show oscillations between the preferred jet tilt of LGM and a more zonal configuration. These switches occur just prior to 19ka BP, sometime between 17 and 16ka BP, and between 15 to 14 ka BP. The first transition occurs within one decade of simulation, while the other two transitions are much more gradual. Finally, the jet shifts away from a preferred tilt position between 12ka BP and 11ka BP, while the range of jet tilt values increases later.

The changes in jet tilt reflect the very different behaviours with time of the upstream (western, 270°E to 300°E) and downstream (eastern, 330°E to 360°E) sides of the NAtl eddy-driven jet, which are outlined by black boxes in Figure 4. Ensemble average changes in jet latitude in the western and eastern regions of the NAtl eddy-driven jet are shown in Figures 10 and 11.

The western side of the jet over NAmer is very focussed and narrowly-distributed, with more than 80% of the winter months spent at the same latitude. The preferred latitude shifts northward twice within a single decade of simulation, at 19.3ka BP and 14.6ka BP. The timing of these transitions match the more gradual shifts in the jet as a whole and two occasions when the tilt is reduced. They are also consistent with the historical timing of the start of the OD and B-A. The transition away from a

Clim. Past Discuss., https://doi.org/10.5194/cp-2018-153
Manuscript under review for journal Clim. Past
Discussion started: 21 November 2018

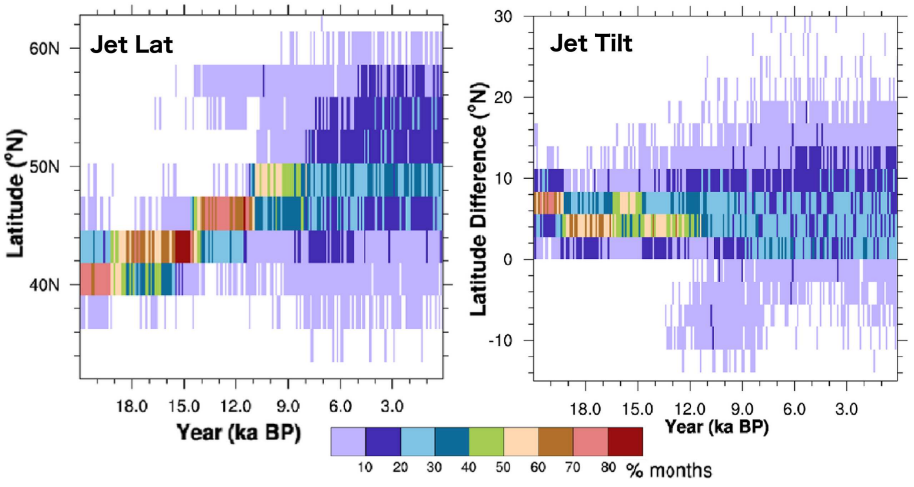

Figure 9. Frequency maps of NAtl, lower-level, jet latitudes and tilt in 10 successive winter seasons accumulated over all ensemble members of the FullyTrans experiment. Colours indicate the percentage of months with peak zonal winds within each latitude bin of width 2.8° at T42.

preferred jet latitude occurs more abruptly than for the jet as a whole at 10.9ka BP. The steady, focussed nature of the western side of the jet under glacial conditions increases its importance for Sverdrup transport in the surface ocean, and conversely, as it becomes more latitudinally-variable, its effectiveness in generating a net transport in the surface ocean reduces (Li and Born). Thus, both the shifting of the focussed, western jet northward and its move to a more broadly-distributed state have important implications for the wind-driven ocean circulation of the NAtl.

In contrast, the eastern side of the jet over the eastern NAtl is less focussed, with the jet occupying its preferred latitude 50 to 60% of the time. There is a single northward shift in the eastern region, occurring more gradually than on the west, between 16 and 15ka BP. This change is a little later than the time of increasing jet tilt. The eastern side of the jet moves away from any preferred latitude between 12ka BP and 11ka BP.

3.3 Attributing causes of simulated jet transitions

In order to attribute the deglacial jet changes to boundary condition changes, we turn to the sensitivity experiments. Since the sources and characteristics of the variations on the western and eastern sides of the jet differ, we present the results of the sensitivity experiments separately for these two regions in Figures 10 and 11. This separation makes it much easier to identify what changes are occurring and attribute their causes than examinations of the mean jet position over the entire range or its tilt, where the influences on the western and eastern sides are mixed. As such, we argue that analyses over these separate regions are more instructive than the standard position and tilt metrics, and would encourage other authors to present these metrics instead. For those interested, sensitivity results for the mean jet position and tilt are presented in Supplemental Figures S5 and S6.

Clim. Past Discuss., https://doi.org/10.5194/cp-2018-153
Manuscript under review for journal Clim. Past
Discussion started: 21 November 2018

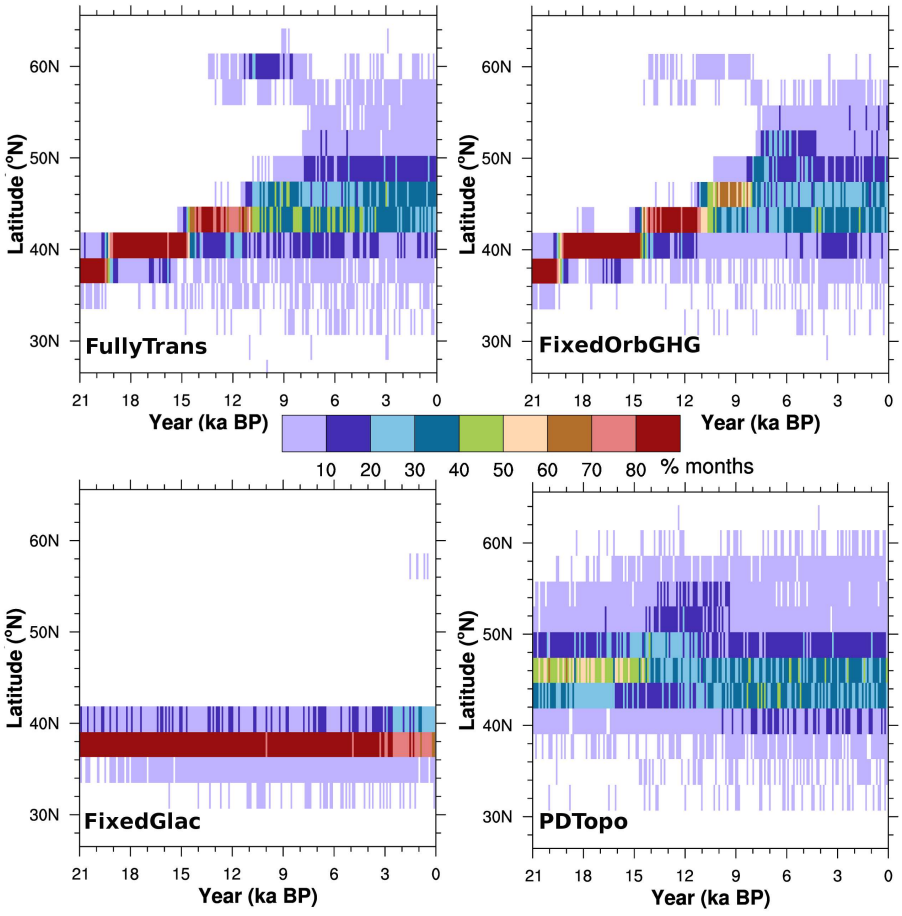

Figure 10. Frequency maps of NAtl, lower-level, western jet latitudes in 10 successive winter seasons accumulated over all ensemble members of the FullyTrans, FixedOrbGHG, FixedGlac and PDTopo experiments. Colours indicate the percentage of months with peak zonal winds within each latitude bin of width 2.8° at T42.

Simulations with fixed LGM ice sheets (FixedGlac in Figures 10 and 11) reproduce neither the deglacial changes to mean jet latitude nor the bulk of changes to its variability on the western and eastern sides of the jet. This effect is most prominent for the western side of the jet, which shows very little change over the deglaciation when the ice sheets are fixed. In contrast, while the eastern jet favoured position does not change under fixed LGM ice sheets, its variability does increase in response to the orbital and greenhouse gas changes. The component of the ice sheets that appears most important to this effect is their elevation, as simulations with infinitessimally-thin but extensive ice sheets (PDTopo) are unable to reproduce the narrow, equatorward-shifted jet seen at LGM in the FullyTrans runs or throughout the FixedGlac runs. Further experiments are required to discern the importance of orography in particular regions of the ice sheets to the jet characteristics. Yet, a relationship can be identified between the latitude of the western side of the jet and the minimum latitude of the south-eastern margin of the NAIS in scatter plots based on the FullyTrans experiments (Figure 12).

Clim. Past Discuss., https://doi.org/10.5194/cp-2018-153
Manuscript under review for journal Clim. Past
Discussion started: 21 November 2018

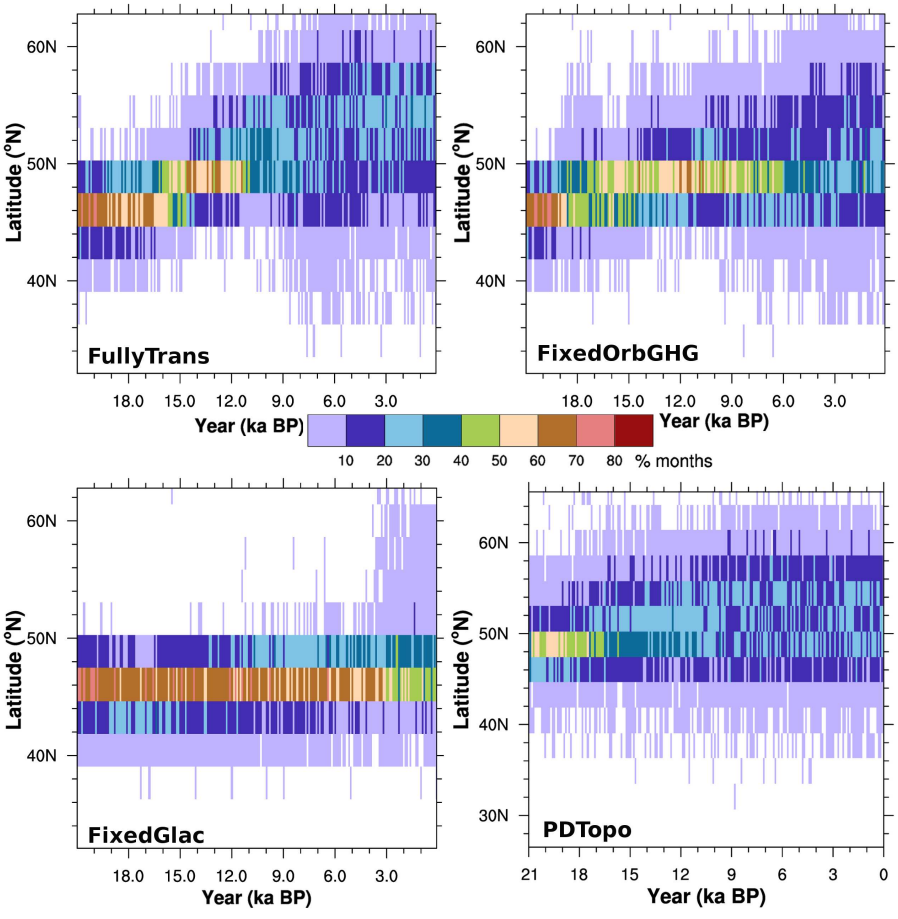

Figure 11. Frequency maps of ensemble-average, NAtl, lower-level, eastern jet latitude in 10 successive winter seasons for FullyTrans, FixedOrbGHG, FixedGlac, and PDTopo experiments. Colours indicate the percentage of months with the difference in jet latitudes between 330°E to 360°E and 270°E to 300°E within each bin of width 2.8°.

The western side of the jet lies south of the 725m contour along the south-eastern NAIS margin at all times in the FullyTrans simulations. The only exception to this is when the wind branch along the north-eastern slope of the NAIS is identified by the algorithm as having the fastest winds (points located within the blue box in Figure 12). There is no such clear relationship with the latitude of the eastern side of the jet (not shown), nor with the latitude of the western side of the jet when the ice sheet is infinitessimally thin in PDTopo. Thus, it appears that the elevated southern margin of the NAIS acts as a physical barrier to the eddies and restricts the positioning of the jet on its northern side. Additional evidence for this is found in the fact that two other simulations generated using PlaSim under different background conditions (i.e. starting from a warmer state and without acceleration, described in Appendices A1 and A2) show western jet shifts at the same time as the FullyTrans simulations. Yet, the jet does not always move to the latitude of the jet. This may be due to other controls on the western side of the jet restricting

Clim. Past Discuss., https://doi.org/10.5194/cp-2018-153
Manuscript under review for journal Clim. Past
Discussion started: 21 November 2018

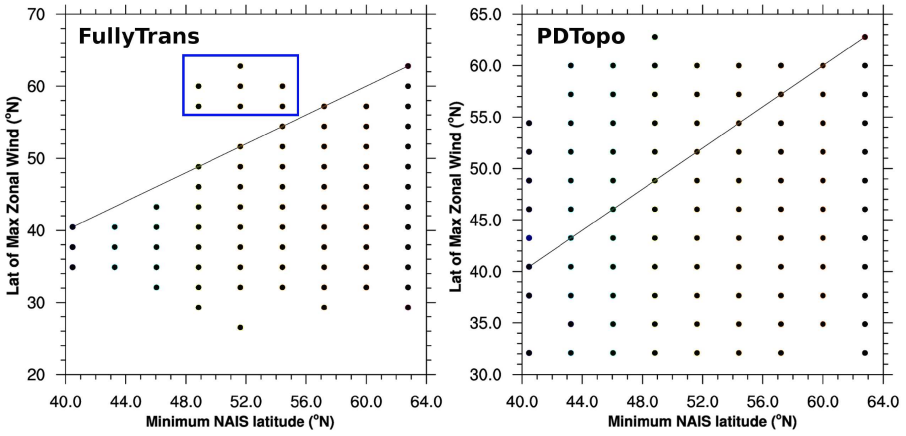

Figure 12. Scatter plots for monthly NAtl jet latitudes on the western side of the Atlantic (270°E - 300°E) versus the minimum latitude of the 725m contour line of the NAIS east of 260°E for all FullyTrans and PDTopo ensemble members. Note these latitudes are calculated on the T42 grid. The blue box identifies points associated with the northern jet latitude branch.

its movement, or more likely, that the barrier effect of the elevation depends on the pressure level at which it is applied (and the vertical profile of pressure will change over the deglaciation).

The consequences of this restriction are that the western end of the jet is more focussed relative to the eastern side, particularly when the NAIS extends well into the midlatitudes, and that the northern range of the western side of the jet increases much more over the deglaciation than its southern range. No ice sheet provides such a restriction to the eastern side of the jet, so the jet in this region is never as focussed as in the west and is more symmetrical in its distribution. The absence of this barrier effect in the PDTopo experiment in Figure 10 is characterized by a more northern position for the preferred jet latitude in the early part of the deglaciation, a lower frequency of time spent at the preferred position, and a broader distribution of values. The preferred tilt in the PDTopo experiment is near zero, as the positions of the western and eastern sides of the jet appear to coincide and shift together.

Ice sheet orography does not provide the only controls on the jet. Fixing the radiative forcings to their LGM values (FixedOrbGHG in Figures 10 and 11) delays the transition away from a strongly preferred jet latitude on both sides of the NAtl eddy-driven jet. The timing of the original two western jet latitude shifts are unaffected by changes to the radiative forcings, although an additional shift occurs after 11ka BP when the radiative forcings are fixed. In contrast, the shift in latitudes occurs earlier on the eastern side of the jet, and no further change to the preferred range of jet latitudes occurs following this. Additionally, the changing radiative forcings in FixedGlac increases the total latitudinal range on the eastern side of the jet and reduces the frequency of the preferred jet location after 4ka BP. Thus, changes to the western side of the jet appear to be predominantly controlled by changes to the position of the southern NAIS margin, while the position of the eastern side of the jet are sensitive to the thermal background conditions of the climate.

Clim. Past Discuss., https://doi.org/10.5194/cp-2018-153
Manuscript under review for journal Clim. Past
Discussion started: 21 November 2018

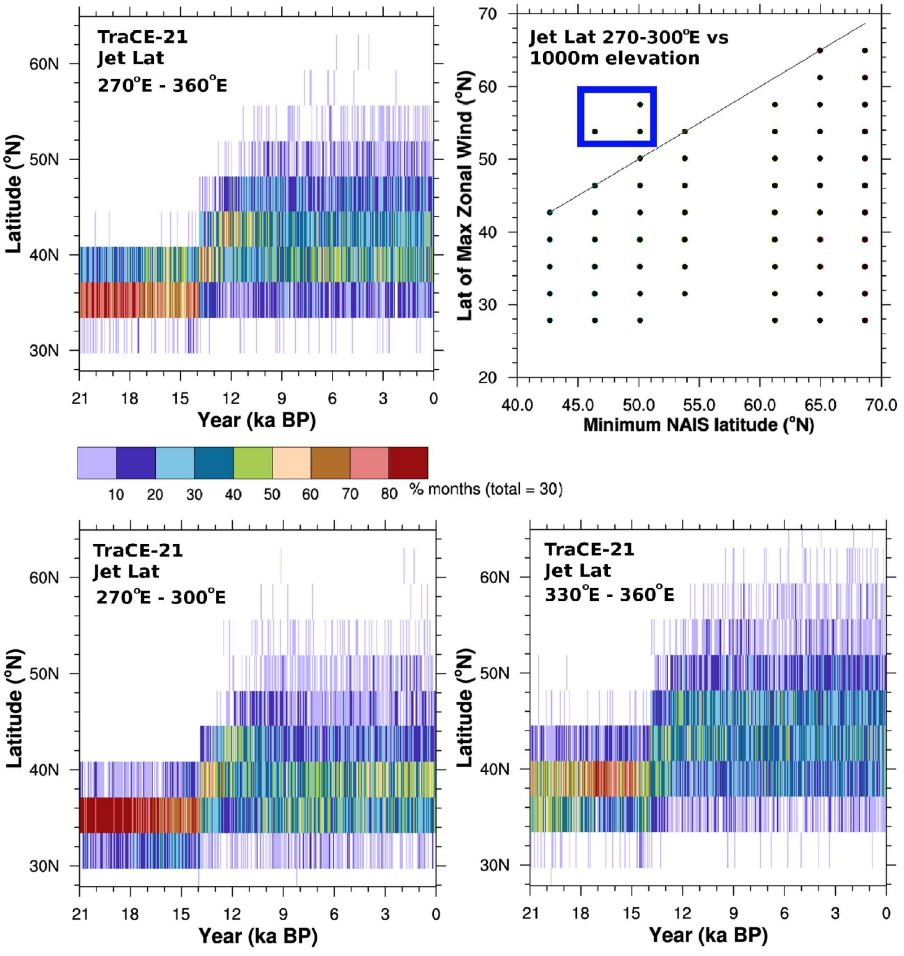

Figure 13. Frequency maps for the NAtl jet derived from the TraCE-21ka deglacial experiment for jet latitudes evaluated over longitudes 270°E to 360°, as well as the upstream (270°E-300°E) and downstream (330°E-360°E) regions. Additionally, a scatter plot is presented of NAtl jet latitudes from the upstream end versus NAIS latitude evaluated as the minimum latitude of the 1000m elevation contour between 260°E to 315°E. A blue box outlines points where winds along the northern slope of the NAIS are stronger than those along its southern margin.

3.4 TraCE-21ka

It is unclear the extent to which the results presented so far are model specific. As a test of their generality, we compare these results against those calculated similarly from the TraCE-21ka experiment, which are plotted in Figure 13.

The NAtl eddy-driven jet in the TraCE-21ka experiment reproduces many of the phenomena observed in the PlaSim simulations, but the details of timing and order differ. At LGM, the jet is highly focussed with a narrow range of values. Its primary latitude shifts northward two times over the deglaciation, and its range increases and preference for a particular latitude de-

Clim. Past Discuss., https://doi.org/10.5194/cp-2018-153
Manuscript under review for journal Clim. Past
Discussion started: 21 November 2018

creases. Unlike the PlaSim simulations, the first transition occurs abruptly at 13.87 ka BP, which coincides with a change in the ice sheet boundary conditions provided to the model. The second transition is much more gradual and occurs at approximately 13ka BP. The first transition is associated with a change on the western side of the jet, whereas the second transition appears to be an artifact of more gradual and asynchronous changes in the western and eastern sides of the jet. The transition away from the jet occupying any latitude more than 50% of the time occurs earlier than in the PlaSim simulations, by 11ka BP, and the range of jet values increases from then until 6ka BP.

The scatter plot in Figure 13 shows that the western side of the NAtl eddy-driven jet does not move north of the 1000m elevation level of the NAIS in eastern NAmer. As with the PlaSim simulations, the only exceptions to this are months when the winds south of the ice sheet are weaker than those north of the ice sheet. The ice sheet height threshold required here is higher than that in the PlaSim simulations, whose threshold is closer to 725m. Given the differences in horizontal and vertical resolution between these two models and that the barrier is likely enacted via a pressure threshold rather than an elevation, such a threshold difference is not unexpected. However, the fact that both models exhibit a strong relationship between winds over eastern NAmer and the regional minimum ice sheet latitude indicates that changes to the position of the jet in this region can be somewhat predictable. From these results, we hypothesize that different ice sheet reconstructions represented at different resolutions will lead to different timings and numbers of jet shifts, but that the jet over the western side of the NAtl will tend to follow the advance and retreat of the southern margin of the NAIS until the margin is sufficiently far north to not interfere with the jet's preferred position. If this hypothesis is correct and this mechanism is as important in reality as it is in models, then the uncertainty in our understanding of the historical position of the jet over eastern NAmer during this period is dominated by the uncertainty in our knowledge of the southernmost position of regional 1000 m (or so) high ice.

Lofverstrom and Lora (2017) diagnose that the eastern side of the NAtl jet in the TraCE-21ka experiment exhibits a rapid northward shift at 13.89ka BP, which they attribute to the separation of the Laurentide and Cordilleran ice domes within the NAIS. This leads to an abrupt increase in jet tilt. There is no such increase in tilt detected in the PlaSim simulations, which may be partly explained by a difference in the longitudes over which the tilt is calculated in this study compared to theirs. Instead, we detect a change in the frequency of time that the jet spends in its preferred location: the eastern jet shifts from spending 40-60% of its time near 40°N at 13.87ka BP to spending 30-40% of its time there and 40-60% of its time two grid positions north of there. This change would look like an abrupt northward shift in the mean NAtl jet position in this region.

4 Conclusions

We have diagnosed winter eddy-driven jet changes in the North Atlantic over the last deglaciation along with some of their controls through the use of a small ensemble of transient simulations using the PlaSim model and the TraCE-21ka simulation. Our main context is the potential for these changes in the jet to contribute to the abrupt climate changes detected in Greenland ice cores and elsewhere. The expected means by which the jet could contribute to abrupt deglacial climate changes is through the influence of winds on surface ocean circulation patterns (and thereby deepwater formation) and on wintertime sea ice extent. Surface ocean circulation patterns are expected to be particularly sensitive to changes in the variability of low-level

winds in the North Atlantic and both components are sensitive to changes in the mean latitudinal position of these winds. We have shown that both of these types of changes occur independently in our simulations. We detect multiple transitions in the mean latitude of the North Atlantic eddy-driven jet over the last deglaciation as well as a more gradual change in its variability.

During the last deglaciation, the North Atlantic eddy-driven jet in the PlaSim simulations makes three distinct steps in latitude at 19ka BP, 14ka BP and at 11ka BP. The first two of these shifts are driven by changes in the position of peak winds on the upwind region of the eddy-driven jet over eastern North America. Only a single shift in peak winds between 16 and 14ka BP is evident in the downstream region of the eddy-driven jet over the eastern side of the North Atlantic. Thus, the tilt of the jet, diagnosed as the difference in the jet position between these two regions, oscillates between values of approximately 8° and 5° according to the asynchronicity of their shifts. The timings of the latitudinal shifts in the western region of the jet are consistent between: the accelerated simulations, an unaccelerated run, and an accelerated transient simulation starting from a warmer initial state. The abruptness of the diagnosed shifts are likely an artifact of the spatial discretization of the model grid, but the two shifts on the western side of the jet both occur within a decade of simulation (a century of forcing). In contrast, the shift on the eastern side of the jet occurs over 200 simulation years (two millennia of forcing), and its timing differs between runs with and without acceleration and in the warmer transient simulation.

The TraCE-21ka experiment also exhibits shifts in the preferred position of the jet, particularly on the western side of the jet. The shifts in the western jet occur at 13.87ka BP and 13ka BP, with the first transition occurring within a single year of a change in the ice sheet boundary condition and with the introduction of anomalous freshwater into the Nordic Seas and St. Lawrence River. The second transition is more gradual.

The variability of the North Atlantic eddy-driven jet changes from a latitudinally-constrained regime to one with a high degree of latitudinal variability over the deglaciation in both datasets. This transition is difficult to date, since it occurs gradually. It is identified through two phenomena: the range of positions occupied by the jet expands over time, and the frequency that the jet occupies its most likely position decreases. The first change occurs in all runs between 11 and 10 ka BP, but only after 8ka BP on the jet's western side. The second change is less distinct and is complete (highest likelihood at any latitude less than 50%) by 8ka BP.

Due to the differences in characteristics of the jet on its western side over eastern North America and its eastern side over the eastern North Atlantic, we attribute the jet changes in these two regions separately. Orbital and greenhouse gas forcings contribute to the spreading of the distribution of jet latitudes away from its peak value in both regions of the jet. However, this effect is most prominent in the eastern North Atlantic, where these forcings also affect the jet's latitudinal position after the deglaciation.

The orography of the ice sheets plays a dominant role over jet changes in both regions; the preferred jet position remains fixed to its value at LGM in both regions in the sensitivity experiment with constant LGM ice topography. For low-level winds over eastern North America, it is the orography of the south-eastern margin that appears to play the most important role, as it acts as a physical barrier for winds in that region in both the PlaSim simulations and the TraCE-21ka experiment. Thus, the western side of the jet is found to be highly-focussed to the latitude of the ice sheet margin and varying only south of the margin until the ice sheet retreats north of the jet's preferred position. In contrast, the downstream side of the jet over the eastern North

Clim. Past Discuss., https://doi.org/10.5194/cp-2018-153
Manuscript under review for journal Clim. Past
Discussion started: 21 November 2018

Atlantic does not show the same sensitivity to marginal position of the North American ice complex and responds to other characteristics of the elevated ice sheet instead. Precisely which characteristics are most important to the jet in this eastern region is not apparent from this study, so we leave that for future work.

The dependence of the jet's western position on the position of the ice sheet margin suggests that deglacial jet changes in this region can be reconstructed from a knowledge of the ice sheet changes. Conversely, the sensitivity of the jet position on the eastern side of the North Atlantic to the background climate state implies that it would be difficult to estimate historical changes to the jet in this region from model simulations, since estimates would vary between models and between simulations with different boundary conditions.

Finally, the simulations presented here did not exhibit abrupt changes in surface temperatures at the times they occurred in the historical record. However, the results provide some insight into what conditions would be required in order for the jet changes detected here to play either a causal or enabling role in abrupt deglacial climate changes. Due to the constraint provided by the ice sheet on the western side of the jet, abrupt changes in this region would most likely arise through one of two phenomena:

1. the ice sheet margin exhibiting an abrupt retreat or abrupt thinning, allowing the jet over the western NAtl to abruptly shift northward, or

2. other processes constraining the regional jet position for an interval of time, allowing a rapid adjustment of the jet to the ice sheet margin, the origin of which are not presently clear.

It is unlikely to see relevant changes in the ice sheet margin occurring on timescales of decades, so it appears that changes to the upstream end of the North Atlantic jet are more likely to play an enabling role than a causal role for abrupt climate oscillations. In contrast, the downstream (eastern) side of the jet exhibits the potential for non-linear behaviour through its sensitivity to the many different components that define the background climate state, including the sea ice extent, sea surface temperatures, and temperature contrasts with the ice sheet and elsewhere. Better understanding the sensitivities of the downstream jet changes will require testing with more sophisticated models that include dynamic sea ice.

5 Acknowledgements

Code availability.

Data availability.

Code and data availability.

Clim. Past Discuss., https://doi.org/10.5194/cp-2018-153
Manuscript under review for journal Clim. Past
Discussion started: 21 November 2018

Climate of the Past Discussions

Sample availability.

Appendix A: Testing Experimental Design

There are two aspects to the design of this study which could possibly affect the results presented here. These include the model's high-latitude cold bias with respect to CMIP5 LGM simulations (described in Section 2.2.5), and the acceleration of the forcings by a factor of 10. The effects of each of these aspects have been assessed using additional simulations and are discussed below.

A1 Cold Arctic at LGM

As described in Section 2.2.5, the PlaSim simulations exhibit colder conditions in the polar regions during winter compared to the CMIP5 multi-model ensemble, particularly in the Northern Hemisphere. The strength of these temperature differences decreases over the deglaciation until by the last millennium the 2m temperatures generated by PlaSim lie mostly within the range of CMIP5 experiments. The location of the largest temperature differences over snow-covered regions suggests that the treatment of snow albedo may at least partly explain them.

Most high-latitude land is covered with a perennial snow cover in the LGM simulations that is metres thick. The albedo of snow in PlaSim is treated as a linear function of surface temperature with cutoff minimum and maximum values of 0.4 and 0.8, respectively. Most problematically, PlaSim's default albedo scheme allows the snow albedo to return to fresh snow values after periods of snow melt, without the requirement of additional snowfall. This unphysical albedo scheme was tested in Koltzow (2007) using the HIRHAM model, and it was found to underestimate satellite-derived clear-sky snow albedo at temperatures above -6°C and overestimate the albedo at temperatures below -8°C. These characteristics are consistent with the climate differences detected in the PlaSim simulations for LGM: they are strongest over snow-covered regions during cold seasons.

To test the influence of this bias, we modified the snow albedo scheme in unforested regions in a manner analogous to Helsen et al. (2017). After a snowfall of at least 20 cm water equivalent, the snow albedo is reset to a maximum value of 0.85. With less snowfall than that, the increase in albedo is scaled linearly between its maximum value and its previous value according to the relative amount of snowfall. When there has been no snowfall, the snow begins to age via an exponential decay via a temperature-dependent time constant toward a temperature-dependent minimum albedo value. This value ranges linearly between an upper limit for firn (albedo 0.75) at temperatures below -5°C and a lower limit for wet snow (albedo 0.55) at temperatures above the melt temperature. The time constant for this decay is defined in Equation A1, where tau is the time constant in days and T is the surface temperature in Kelvin.

$$\tau = 30 - 29.875 * MIN[1, MAX[0, ((T - 268.16)/(273.15 - 268.16))^{0.25}]] \quad \text{(A1)}$$

This parametrization of the time constant gives values of 3 hours for temperatures at the melting point, 4 days for -2°C and 30 days for -5°C.

Clim. Past Discuss., https://doi.org/10.5194/cp-2018-153
Manuscript under review for journal Clim. Past
Discussion started: 21 November 2018

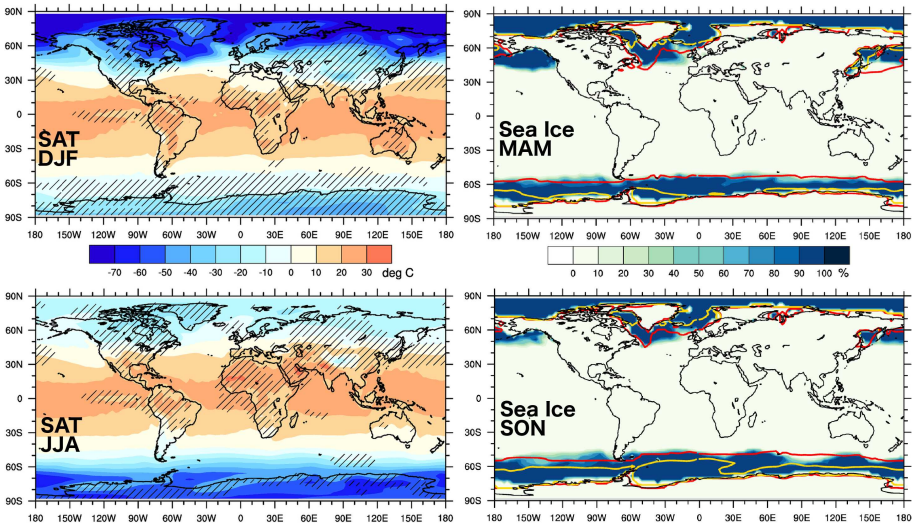

Figure A1. 2-metre temperatures and sea ice concentration at LGM in the first century of a single transient simulation employing the new snow albedo parametrization compared to CMIP5 multi-model minimum and maximum values. Hatching represents regions where climatological values lie within the range of CMIP5 models, while red lines indicate CMIP5 maximum sea ice extent and yellow lines indicate CMIP5 minimum extent.

This updated snow albedo parametrization was applied in PlaSim to snow cover over land and sea ice, and a new LGM spin-up and accelerated transient experiment were performed. Sea ice is much less extensive at LGM in the new transient simulation as seen in Figure A1 and temperature biases with respect to the CMIP5 multi-model ensemble are reduced. However, Arctic winter temperatures are still outside the range of the CMIP5 models at LGM. The remaining model differences suggest the need for additional comparisons in the tuning procedure that constrain the seasonal cycle, which would better constrain the changes in the climate under different forcing conditions.

The jet latitudes in the transient run using the new albedo parametrization are very similar to those in the original accelerated transient simulations in the upstream region of the jet. However, in the jet as a whole and in the downstream regions plotted in Figure A2, the transition to a more distributed jet without a single preferred latitude over the eastern NAtl occurs much earlier, by 15ka BP instead 11ka BP. These changes are consistent with the conclusions presented here that the constraints on the upstream end of the jet are primarily caused by the position of the south-eastern margin of the NAIS, while the controls on the east are based on the thermal state of the atmosphere and sea surface temperatures. A warmer initial state with less extensive sea ice achieves a similar jet state over the eastern NAtl earlier.

A2 Simulation Acceleration

Another run was generated identical to FullyTrans1 except without acceleration to identify what influence the ten times acceleration may have had on the results presented here and to better assess the abruptness of the transitions. Frequency plots for

Clim. Past Discuss., https://doi.org/10.5194/cp-2018-153
Manuscript under review for journal Clim. Past
Discussion started: 21 November 2018

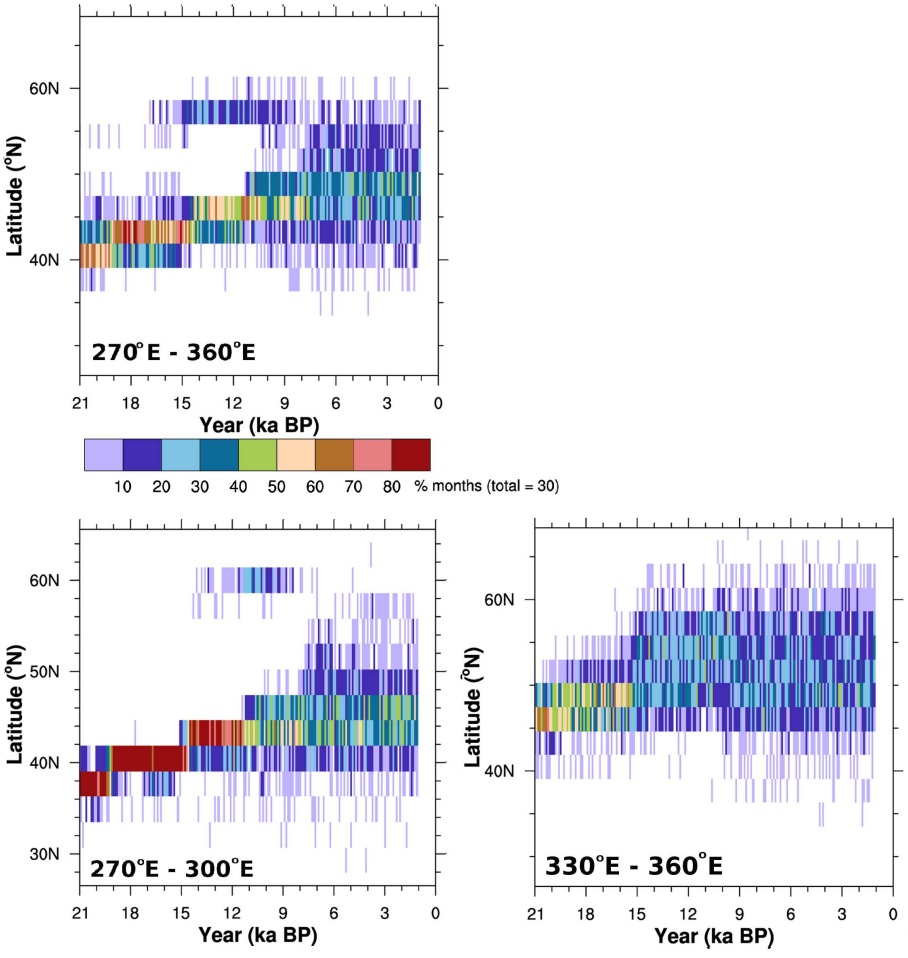

Figure A2. Frequency plots for North Atlantic eddy-driven jet latitudes as a function of time for the transient deglacial simulation using a revised snow albedo parametrization.

the jet latitudes in all regions are shown to year 6.3ka BP in Figure A3. Jet latitude shifts in the western region of the jet occur at the same time as in the accelerated runs, and the most abrupt transition between 15ka BP and 14ka BP occurs within 80 years. Over the eastern region, the jet changes occur earlier than without acceleration. Thus, allowing the ocean to adjust to the changing climate conditions results in a change to the timing of the shifting of the jet over the eastern NAtl and the shift away from a preferred jet latitude. Notably, there are quasi-periodic, short-lived episodes throughout the deglaciation in this run when the jet position in the east shifts northward, and its range extends much further north. These periods are coincident with episodes of abrupt warming in the run.

Clim. Past Discuss., https://doi.org/10.5194/cp-2018-153
Manuscript under review for journal Clim. Past
Discussion started: 21 November 2018

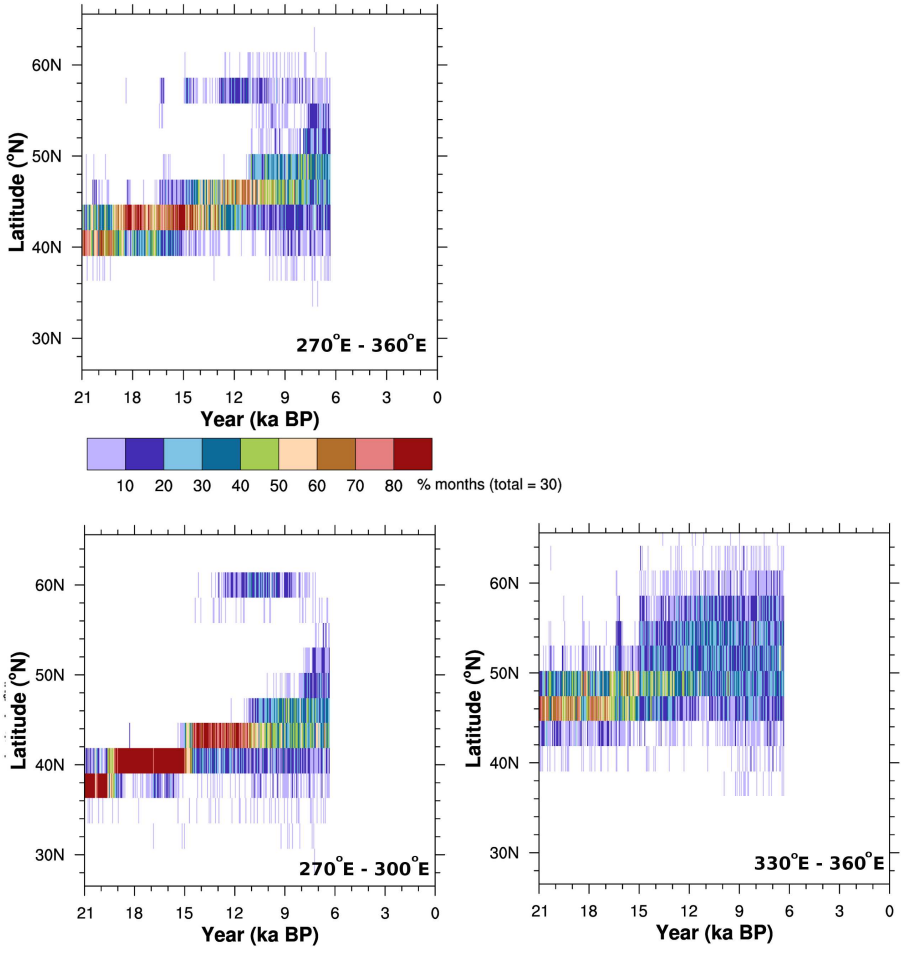

Figure A3. Frequency plots for North Atlantic eddy-driven jet latitudes as a function of time for the unaccelerated transient deglacial simulation.

Author contributions. HJA and LT designed the experiments. HJA modified the PlaSim model code, performed the simulations and analysed the output. HJA prepared the manuscript with contributions from LT.

Competing interests. The authors declare that they have no conflict of interest.

Disclaimer.

Clim. Past Discuss., https://doi.org/10.5194/cp-2018-153
Manuscript under review for journal Clim. Past
Discussion started: 21 November 2018

Acknowledgements. The authors thank Camille Li for her insightful comments and Taimaz Bahadory for his editing. Funding for HJA was provided by ArcTrain Canada and the German Federal Ministry of Education and Research (BMBF) in its Research for Sustainability initiative (FONA) through the PalMod project. All calculations were performed using HPC services from the Centre for Health Informatics and Analytics at the Memorial University of Newfoundland. TraCE-21ka was made possible by the DOE INCITE computing program, and supported by NCAR, the NSF P2C2 program, and the DOE Abrupt Change and EaSM programs.

Clim. Past Discuss., https://doi.org/10.5194/cp-2018-153
Manuscript under review for journal Clim. Past
Discussion started: 21 November 2018

Climate of the Past Discussions
Open Access
EGU

References

Arbuszewski, J. A., deMenocal, P. B., Cléroux, C., Bradtmiller, L., and Mix, A.: Meridional shifts of the Atlantic intertropical convergence zone since the Last Glacial Maximum, Nature Geoscience, 6, 959–962, https://doi.org/10.1038/NGEO1961, 2013.

Barnes, E. A. and Hartmann, D. L.: Rossby wave scales, propagation, and the variability of eddy-driven jets, Journal of the Atmospheric Sciences, 68, 2893–2908, https://doi.org/10.1175/JAS-D-11-039.1, 2011.

Berger, A. L.: Long-term variations of daily insolation and Quaternary climatic changes, Journal of the Atmospheric Sciences, 35, 2362–2367, 1978.

Blunier, T., Chappellaz, J., Schwander, J., Dallenbach, A., Stauffer, B., Stocker, T. F., Raynaud, D., Jouzel, J., Clausen, H. B., Hammer, C. U., and Johnsen, S. J.: Asynchrony of Antarctic and Greenland climate change during the last glacial period, Nature, 394, 739–743, 1998.

Bradley, R. S. and England, J. H.: The Younger Dryas and the sea of ancient ice, Quaternary Research, 70, 1–10, https://doi.org/10.1016/j.yqres.2008.03.002, 2008.

Briggs, R., Pollard, D., and Tarasov, L.: A glacial systems model configured for large ensemble analysis of Antarctic deglaciation, The Cryosphere, 7, 1949–1970, https://doi.org/10.5194/tc-7-1949-2013, 2013.

Briggs, R., Pollard, D., and Tarasov, L.: A data-constrained large ensemble analysis of Antarctic evolution since the Eemian, Quaternary Science Reviews, 103, 91–115, https://doi.org/10.1016/j.quascirev.2014.09.003, 2014.

Broecker, W. S., Kennett, J. P., adn James T. Teller adn Sue Trumbore, B. P. F., Bonani, G., and Wolfli, W.: Routing of meltwater from the Laurentide Ice Sheet during the Younger Dryas cold episode, Nature, 341, 318–321, 1989.

Clark, P. U., Shakun, J. D., Baker, P. A., Bartlein, P. J., Brewer, S., Brook, E., Carlson, A. E., Cheng, H., Kaufman, D. S., Liu, Z., Marchitto, T. M., Mix, A. C., Morrill, C., Otto-Bliesner, B. L., Pahnke, K., Russell, J. M., Whitlock, C., Adkins, J. F., Blois, J. L., Clark, J., Colman, S. M., Curry, W. B., Flower, B. P., He, F., Johnson, T. C., Lynch-Stieglitz, J., Markgraf, V., McManus, J., Mitrovica, J. X., Moreno, P. I., and Williams, J. W.: Global climate evolution during the last deglaciation, Proceedings of the North American Society, 109, E1134–E1142, https://doi.org/10.1073/pnas.1116619109, 2012.

Cohen, J., Screen, J. A., Furtado, J. C., Barlow, M., Whittleston, D., Coumou, D., Francis, J., Dethloff, K., Entekhabi, D., Overland, J., and Jones, J.: Recent Arctic amplification and extreme mid-latitude weather, Nature Geoscience, 7, 627–637, https://doi.org/10.1038/NGEO2234, 2014.

Cook, K. H. and Held, I. M.: Stationary waves of the ice age climate, Journal of Climate, 1, 807–819, 1988.

Dyke, A. S.: An outline of North American deglaciation with emphasis on central and northern Canada, Developments in Quaternary Sciences, 2, 373–424, 2004.

Gherardi, J.-M., Labeyrie, L., Nave, S., Francois, R., McManus, J. F., and Cortijo, E.: Glacial-interglacial circulation changes inferred from $^{231}Pa^{230}Th$ sedimentary record in North Atlantic region, Paleoceanography, 24, PA2204, https://doi.org/10.1029/2008PA001696, 2009.

Grachev, A. M. and Severinghaus, J. P.: A revised $+10\pm4^{o}C$ magnitude of the abrupt change in Greenland temperature at the Younger Dryas termination using published GISP2 gas isotope data and air thermal diffusion constants, Quaternary Science Reviews, 24, 513–519, https://doi.org/10.1016/j.quascirev.2004.10.016, 2005.

Häkkinen, S., Rhines, P. B., and Worthen, D. L.: Atmospheric blocking and Atlantic multidecadal ocean variability, Science, 334, 655–670, https://doi.org/10.1126/science.1205683, 2011.

Hammer, C. U., Clausen, H. B., and Tauber, H.: Ice-core dating of the Pleistocene/Holocene boundary applied to a calibration of the $^{1}4C$ time scale, Radiocarbon, 28, 284–291, 1986.

He, F.: Simulating transient climate evolution of the last deglaciation with CCSM3, Ph.D. thesis, University of Wisconsin-Madison, http://www.cgd.ucar.edu/ccr/TraCE/doc/He_PhD_dissertation_UW_2011.pdf, 2011.

Helsen, M. M., van de Wal, R. S. W., Reerink, T. J., Bintanja, R., Madsen, M. S., Yang, S., Li, Q., and Zhang, Q.: On the importance of the albedo parameterization for the mass balance of the Greenland ice sheet in EC-Earth, The Cryosphere, 11, 1949–1965, https://doi.org/10.5194/tc-11-1949-2017, 2017.

Hu, A., Meehl, G. A., Otto-Bliesner, B. L., Waelbroeck, C., Han, W., Loutre, M.-F., Lambeck, K., Mitrovica, J. X., and Rosenbloom, N.: Influence of Bering Strait flow and North Atlantic circulation on glacial sea-level changes, Nature Geoscience, 3, 118–121, https://doi.org/10.1038/NGEO729, 2010.

Hughes, A. L. C., Gyllencreutz, R., Lohne, O. S., and adn John Inge Svendsen, J. M.: The last Eurasian ice sheets - a chronological database and time-slice reconstruction, DATED-1, Boreas, 45, 1–45, https://doi.org/10.1111/bor.12142, 2016.

Ivanovic, R. F., Gregoire, L. J., Kageyama, M., Roche, D. M., Valdes, P. J., Burke, A., Drummond, R., Peltier, W. R., and Tarasov, L.: Transient climate simulations of the deglaciation 21-9 thousand years before present (version 1) - PMIP4 Core experiment design and boundary conditions, Geoscientific Model Development, 9, 2563–2587, https://doi.org/10.5194/gmd-9-2563-2016, 2016.

Jacob, J., Huang, Y., Disnar, J.-R., Sifeddine, A., Boussafir, M., Albuquerque, A. L. S., and Turcq, B.: Paleohydrological changes during the last deglaciation in Northern Brazil, Quaternary Science Reviews, 26, 1004–1015, https://doi.org/10.1016/j.quascirev.2006.12.004, 2007.

Justino, F., Timmermann, A., Merkel, U., and Souza, E. P.: Synoptic reorganization of atmospheric flow during the Last Glacial Maximum, Journal of Climate, 18, 2826–2846, 2005.

Kageyama, M. and Valdes, P. J.: Impact of the North American ice-sheet orography on the Last Glacial Maximum eddies and snowfall, Geophysical Research Letters, 27, 1515–1518, 2000.

Kageyama, M., Paul, A., Roche, D. M., and Meerbeeck, C. J. V.: Modelling glacial climatic millennial-scale variability related to changes in the Atlantic meridional overturning circulation: a review, Quaternary Science Reviews, 29, 2931–2956, https://doi.org/10.1016/j.quascirev.2010.05.029, 2010.

Kageyama, M., Merkel, U., Otto-Bliesner, B., Prange, M., Abe-Ouchi, A., Lohmann, G., Ohgaito, R., Roche, D. M., Singarayer, J., Swingedouw, D., and et al.: Climatic impacts of fresh water hosing under Last Glacial Maximum conditions: a multi-model study, Climate of the Past, 9, 935–953, https://doi.org/10.5194/cp-9-935-2013, http://dx.doi.org/10.5194/cp-9-935-2013, 2013.

Keigwin, L. D., Klotsko, S., Zhao, N., Reilly, B., Giosan, L., and Driscoll, N. W.: Deglacial floods in the Beaufort Sea preceded Younger Dryas cooling, Nature Geoscience, 11, 599–604, https://doi.org/10.1038/s41561-018-0169-6, 2018.

Knorr, G. and Lohmann, G.: Rapid transitions in the Atlantic thermohaline circulation triggered by global warming and meltwater during the last deglaciation, Geochemistry Geophysics Geosystems, 8, Q12 006, https://doi.org/10.1029/2007GC001604, 2007.

Koltzow, M.: The effect of a new snow and sea ice albedo scheme on regional climate model simulations, Journal of Geophysical Research, 112, D07 110, https://doi.org/10.1029/2006JD007693, 2007.

Lee, S. and Kim, H.-K.: The dynamical relationship between subtropical and eddy-driven jets, Journal of the atmospheric sciences, 60, 1490–1503, 2003.

Li, C. and Battisti, D.: Reduced Atlantic storminess during Last Glacial Maximum: evidence from a coupled climate model, Journal of Climate, 21, 3561–3580, https://doi.org/10.1175/2007JCLI2166.1, 2008.

Li, C. and Born, A.: Coupled atmosphere-ice-ocean dynamics in Dansgaard-Oeschger cycles, submitted to Quaternary Science Reviews.

Liu, Z., Otto-Bliesner, B. L., He, F., Brady, E. C., Tomas, R., Clark, P. U., Carlson, A. E., Lynch-Stieglitz, J., Curry, W., Brook, E., Erickson, D., Jacob, R., Kutzbach, J., and Cheng, J.: Transient simulation of last deglaciation with a new mechanism for Bolling-Allerod warming, Science, 325, 310–314, https://doi.org/10.1126/science.1171041, 2009.

Liu, Z., Carlson, A. E., He, F., Brady, E. C., Otto-Bliesner, B. L., Briegleb, B. P., Wehrenberg, M., Clark, P. U., Wu, S., Cheng, J., Zhang, J., Noone, D., and Zhu, J.: Younger Dryas cooling and the Greenland climate response to CO_2, PNAS, 109, 11 101–11 104, https://doi.org/10.1073/pnas.1202183109, 2012.

Lofverstrom, M. and Lora, J. M.: Abrupt regime shifts in the North Atlantic atmospheric circulation over the last deglaciation, Geophysical Research Letters, 44, 8047–8055, https://doi.org/10.1002/2017GL074274, 2017.

Lofverstrom, M., Caballero, R., Nilsson, J., and Kleman, J.: Evolution of the large-scale atmospheric circulation in response to changing ice sheets over the last glacial cycle, Climate of the Past, 10, 1453–1471, https://doi.org/10.5194/cp-10-1453-2014, 2014.

Loulergue, L., Schilt, A., Spahni, R., Masson-Delmotte, V., Blunier, T., Lemieux, B., Barnola, J.-M., Raynaud, D., Stocker, T. F., and Chappellaz, J.: Orbital and millennial-scale features of atmopsheric CH4 over the past 800,000 years, Nature, 453, 383–386, https://doi.org/10.1038/nature06950, 2008.

Lozier, M. S., Roussenov, V., Reed, M. S. C., and Williams, R. G.: Opposing decadal changes for the North Atlantic meridional overturning circulation, Nature Geoscience, 3, 728–735, https://doi.org/10.1038/NGEO947, 2010.

Lunkeit, F., Borth, H., Bottinger, M., Fraedrich, K., Jansen, H., Kirk, E., Kleidon, A., Luksch, U., Paiewonsky, P., Schubert, S., Sielmann, S., and Wan, H.: Planet Simulator reference manual version 16, Tech. rep., University of Hamburg, Hamburg, DE, last Updated: February 6, 2012, 2012.

Luthi, D., Floch, M. L., Bereiter, B., Blunier, T., Barnola, J.-M., Siegenthaler, U., Raynaud, D., Jouzel, J., Fischer, H., Kawamura, K., and Stocker, T. F.: High-resolution carbon dioxide concentration record 650,000-800,000 years before present, Nature, 453, 379–382, https://doi.org/10.1038/nature06949, 2008.

Maier-Reimer, E., Mikolajewicz, U., and Hasselmann, K.: Mean circulation of the Hamburg LSG OGCM and its sensitivity to the thermohaline surface forcing, Journal of Physical Oceanography, 23, 731–757, 1993.

Meinshausen, M., Vogel, E., Nauels, A., Lorbacher, K., Meinshausen, N., Etheridge, D. M., Fraser, P. J., Montzka, S. A., Rayner, P. J., Trudinger, C. M., Krummel, P. B., Beyerle, U., Canadell, J. G., S.Daniel, J., Enting, I. G., Law, R. M., Lunder, C. R., O'Doherty, S., Prinn, R. G., Reimann, S., Rubino, M., Velders, G. J. M., Vollmer, M. K., Wang, R. H. J., and Weiss, R.: Historical greenhouse gas concentrations for climate modelling (CMIP6), Geoscientific Model Development, 10, 2057–2116, https://doi.org/10.5194/gmd-10-2057-2017, 2017.

Merz, N., Raible, C. C., and Woollings, T.: North Atlantic eddy-driven jet in interglacial and glacial winter climates, Journal of Climate, 28, 3977–3998, https://doi.org/10.1175/JCLI-D-14-00525.1, 2015.

Mohtadi, M., Prange, M., and Steinke, S.: Palaeoclimatic insights into forcing and response of monsoon rainfall, Nature, 533, 191–199, https://doi.org/10.1038/nature17450, 2016.

Muglia, J. and Schmittner, A.: Glacial Atlantic overturning increased by wind stress in climate models, Geophysical Research Letters, 42, 9862–9869, https://doi.org/10.1002/2015GL064583, 2015.

Peltier, W. R. and Vettoretti, G.: Dansgaard-Oeschger oscillations predicted in a comprehensive model of glacial climate: A "kicked" salt oscillator in the Atlantic, Geophysical Research Letters, 41, 7306–7313, https://doi.org/10.1002/2014GL061413, 2014.

Peltier, W. R., Argus, D. F., and Drummond, R.: Space geodesy constrains ice age terminal deglaciation: the global ICE-6G_C (VM5a) model, Journal of geophysical research: solid earth, 120, 450–487, https://doi.org/10.1002/2014JB011176, 2015.

Ramaswamy, V., Boucher, O., Haigh, J., Hauglustaine, D., Haywood, J., Myhre, G., Nakajima, T., Shi, G. Y., Solomon, S., Betts, R., Charlson, R., Chuang, C., Daniel, J. S., Genio, A. D., van Dorland, R., Feichter, J., Fuglestvedt, J., de F. Forster, P. M., Ghan, S. J., Jones, A., Kiehl, J. T., Koch, D., Land, C., Lean, J., Lohmann, U., Minschwaner, K., Penner, J. E., Roberts, D. L., Rodhe, H., Roelofs, G. J., Rotstayn, L. D., Schneider, T. L., Schumann, U., Schwartz, S. E., Schwarzkopf, M. D., Shine, K. P., Smith, S., Stevenson, D. S., Stordal, F., Tegen, I., and Zhang, Y.: Radiative forcing of climate change, in: Climate Change 2001: The scientific basis. Contribution of working group I to the Third Assessment Report of the Intergovernmental Panel on Climate Change, edited by Joos, F. and Srinivasan, J., pp. 349–416, Cambridge University Press, 2001.

Renssen, H. and Isarin, R. F. B.: The two major warming phases of the last deglaciation at Ĩ4.7 and Ĩ1.5ka cal BP in Europe: climate reconstructions and AGCM experiments, Global and Planetary Change, 30, 117–153, https://doi.org/10.1016/S0921-8181(01)00082-0, 2001.

Repschläger, J., Weinelt, M., Kinkel, H., Andersen, N., and Garbe-Schönberg, D.: Response of the subtropical North Atlantic surface hydrography on deglacial and Holocene AMOC changes, Paleoceanography, 30, 456–476, https://doi.org/10.1002/2014PA002637, 2015.

Rind, D.: Components of the ice age circulation, Journal of Geophysical Research, 92, 4241–4281, 1987.

Roe, G. H. and Lindzen, R. S.: A one-dimensional model for the interaction between continental-scale ice sheets and atmospheric stationary waves, Climate Dynamics, 17, 479–487, 2001a.

Roe, G. H. and Lindzen, R. S.: The mutual interaction between continental-scale ice sheets and atmospheric stationary waves, Journal of Climate, 14, 1450–1465, 2001b.

Rooth, C.: Hydrology and Ocean Circulation, Progress in Oceanography, 11, 131–149, 1982.

Seager, R. and Battisti, D. S.: Challenges to our understanding of the general circulation: abrupt climate change, in: Global Circulation of the Atmosphere, edited by Schneider and Sobel, pp. 331–371, Princeton University Press, 2007.

Shakun, J. D. and Carlson, A. E.: A global perspective on Last Glacial Maximum to Holocene climate change, Quaternary Science Reviews, 29, 1801–1816, https://doi.org/10.1016/j.quascirev.2010.03.016, 2010.

Tarasov, L. and Peltier, W. R.: Greenland glacial history, borehole constraints and Eemian extent, J. Geophys. Res., 108, 2124–2143, 2003.

Tarasov, L. and Peltier, W. R.: A geophysically constrained large ensemble analysis of the deglacial history of the North American ice-sheet complex, Quaternary Science Reviews, 23, 359–388, https://doi.org/10.1016/j.quascirev.2003.08.004, 2004.

Tarasov, L. and Peltier, W. R.: Arctic freshwater forcing of the Younger Dryas cold reversal, Nature, 435, 662–665, https://doi.org/10.1038/nature03617, 2005.

Tarasov, L., Dyke, A. S., Neal, R. M., and Peltier, W. R.: A data-calibrated distribution of deglacial chronologies for the North American ice complex from glaciological modeling, Earth and Planetary Science Letters, 315-316, 30–40, 2012.

Tarasov, L., Hughes, A., Gyllencreutz, R., Lohne, O. S., Mangerud, J., and Svendsen, J.-I.: The global GLAC-1c deglaciation chronology, melwater pulse 1-a, and a question of missing ice, in: IGS Symposium on Contribution of Glaciers and Ice Sheets to Sea-Level Change, IGS Symposium abstracts, 2014.

Tibaldi, S. and Geleyn, J.-F.: The production of a new orography, land sea mask and associated climatological surface fields for operational purpose, Tech. rep., European Centre for Medium-range Weather Forecasts, https://www.ecmwf.int, 1981.

Venegas, S. A. and Mysak, L. A.: Is there a dominant timescale of natural climate variability in the Arctic?, Journal of Climate, 13, 3412–3434, https://doi.org/10.1175/1520-0442(2000)013<3412:ITADTO>2.0.CO;2, 2000.

Woollings, T., Hannachi, A., and Hoskins, B.: Variability of the North Atlantic eddy-driven jet stream, Quaterly Journal of the Royal Meteorological Society, 136, 857–868, https://doi.org/10.1002/qj.625, 2010.

Clim. Past Discuss., https://doi.org/10.5194/cp-2018-153
Manuscript under review for journal Clim. Past
Discussion started: 21 November 2018

Wunsch, C.: Abrupt climate changes: an alternative view, Quaternary Research, 65, 191–203, https://doi.org/10.1016/j.yqres.2005.10.006, 2006.